

Q

DOCUMENT RESUME

ED 195 412

SE 033 403

AUTHOR Reihman, Thomas C.  
 TITLE Nuclear Engineering Computer Modules, Thermal-Hydraulics, TH-3: High Temperature Gas Cooled Reactor Thermal-Hydraulics.  
 INSTITUTION Virginia Polytechnic Inst. and State Univ., Blacksburg. Coll. of Engineering.  
 SPONS AGENCY National Science Foundation, Washington, D.C.  
 PUB DATE [73]  
 NOTE 119p.: For related documents, see SE 033 401-402. Contains marginal legibility in computer printouts.

EDRS PRICE MF01/PC05 Plus Postage.  
 DESCRIPTORS \*College Science; \*Computer Programs; Engineering; \*Engineering Education; Higher Education; Hydraulics; \*Learning Modules; Mathematical Models; Mechanics (Physics); \*Nuclear Physics; Physics; \*Science Education; Science Instruction; Thermodynamics

ABSTRACT

This learning module is concerned with the temperature field, the heat transfer rates, and the coolant pressure drop in typical high temperature gas-cooled reactor (HTGR) fuel assemblies. As in all of the modules of this series, emphasis is placed on developing the theory and demonstrating its use with a simplified model. The heart of the module is the HTGR Thermal-Hydraulics Computer Code which solves for the radial temperature distributions in the fuel, moderator, and coolant at any axial station and then marches axially with an energy balance in the coolant. The code and its use are described in detail including a listing and definition of all variables, a discussion of all input requirements and resulting output, an annotated flow chart of the code, an explanation of all options in the code, and a listing of the code which gives enough comment statements to clearly indicate the operational steps being performed. By proper specification of the option, the code can either be used as an individual entity to study thermal-hydraulic aspects exclusively, or as a subroutine in the total HTGR module package to provide temperature feedback to the other modules. Examples are worked out using the code. (Author/SK)

\*\*\*\*\*  
 \* Reproductions supplied by EDRS are the best that can be made \*  
 \* from the original document. \*  
 \*\*\*\*\*

THERMAL-HYDRAULICS MODULE, TH-3  
HIGH TEMPERATURE GAS-COOLED REACTOR THERMAL-HYDRAULICS

by

Thomas C. Reihman

The University gratefully acknowledges the support of the  
Division of Higher Education of the National Science Foundation  
for support of this work performed under Grant GZ-2888 and the  
support of Duke Power Company, North Carolina Power and Light Company,  
and Virginia Electric and Power Company.

Project Director: Milton C. Edlund

DEC 12 1980

TABLE OF CONTENTS

	<u>Page</u>
1.0 Object of Module . . . . .	1
2.0 Content of the Module. . . . .	2
3.0 HTGR Fuel Geometry and Its Model . . . . .	4
4.0 HTGR Thermal-Hydraulic Theory. . . . .	8
4.1 Internal Heat Generation . . . . .	8
4.2 Temperature Distribution in the Fuel . . . . .	11
4.3 Temperature Distribution in the Graphite Moderator . . . . .	18
4.4 Temperature Drop in the Convective Layer . . . . .	38
4.5 Pressure Drop in the Coolant . . . . .	40
4.6 The Heat Transfer Coefficient. . . . .	46
4.7 Incremental Energy Balances. . . . .	52
5.0 The HTGR Thermal-Hydraulics Code . . . . .	54
5.1 Nomenclature . . . . .	60
5.2 Code Input . . . . .	65
5.3 Code Output. . . . .	68
5.4 Code Flow Chart. . . . .	69
5.5 Code Examples. . . . .	76
5.6 Listing of Code. . . . .	94
6.0 References . . . . .	.111
7.0 Problems . . . . .	.112

## THERMAL-HYDRAULICS MODULE, TH-3

### HIGH TEMPERATURE GAS-COOLED REACTOR THERMAL-HYDRAULICS

#### 1.0 Object of Module

The object of this module is to present the basic elements of high temperature gas-cooled reactor (HTGR) thermal-hydraulics. This requires the demonstration of:

- How the actual reactor core geometry can be modeled for simplified thermal-hydraulic analysis.
- What information is necessary to characterize the thermal-hydraulic behavior of the reactor.
- The development of the theoretical relations that permit the computation of these thermal-hydraulic characteristics.
- The actual calculation of this information for the reactor. This calculation requires the use of the HTGR Thermal-Hydraulics Code, the description of which is included in this module.

The thermal-hydraulic characteristics of the reactor are required for the determination of:

- Fuel integrity
- Moderator behavior
- Coolant exit conditions
- Helium compressor requirements
- Temperature feedback for reactor neutronics calculations.

## 2.0 Content of the Module

This learning module contains the thermal-hydraulics of high temperature gas-cooled reactors. Specifically, the module is concerned with the temperature field, the heat transfer rates and the coolant pressure drop in typical HTGR fuel assemblies.

As in all of the modules of this series, emphasis is placed on developing the theory and demonstrating its use with a simplified model. The model is carefully selected to insure that analyses based on it will exhibit all of the important thermal-hydraulic trends of the typical reactor. The description of the core of a typical high temperature gas-cooled reactor and the modeling of its thermal-hydraulic characteristics are treated in the next section of this module.

Following the geometry and modeling section, the basic theory governing the temperature distributions, heat transfer rates, pressure drops, and energy balance considerations is presented. The temperature distribution in the fuel is calculated assuming one-dimensional radial heat conduction. In the graphite moderator a two-dimensional finite difference calculation is used. The pressure drop in the coolant channels and the heat transfer coefficient for use in Newton's law of cooling are calculated from empirical relations developed for reactor coolant channel flows. Energy balances for small axial segments of the coolant channel are used to step the solution in the axial direction. Simple examples, illustrating the individual calculations, are worked out in detail for typical HTGR conditions.

The heart of the module is the HTGR Thermal-Hydraulics Computer Code. Basically, the code solves for the radial temperature distributions in the fuel, moderator, and coolant at any axial station and then marches

axially with an energy balance in the coolant. The code and its use are described in detail. Included are a listing and definition of all variables, a discussion of all input requirements and resulting output, an annotated flow chart of the code, an explanation of all options in the code, and a listing of the code which includes enough comment statements to clearly indicate the operational steps being performed. By proper specification of the options the code can either be used as an individual entity to study thermal-hydraulic aspects exclusively or as a subroutine in the total HTGR module package to provide temperature feedback to the other modules. Examples are worked out using the code. In typical examples, the location and magnitude of the maximum fuel temperature in the HTGR are found and the effect of undersized coolant flow channels on maximum fuel temperature and coolant outlet temperature are determined.

### 3.0. HTGR Fuel Geometry and Its Model

The typical high temperature gas-cooled reactor core is approximately cylindrical in shape. A unit producing 3000 Mw(t) is composed of about 4000 fuel element assemblies. These fuel element assemblies are in the shape of right hexagonal prisms about 31 in. high and about 14 in. across the flats. The fuel element assemblies are arranged in about 500 stacks, each 8 elements high, to form a core about 27 ft in diameter and 21 ft high. To provide a flattening of the neutron flux (and hence the power production) in the radial direction, the enrichment of the fuel in the fuel element assemblies is varied in cylindrical zones. Dowels are used to precisely align the fuel element assemblies. A small gap (about 0.04 in.) exists between the elements at room temperature to accommodate thermal expansion. The core is surrounded by reflector and containment components which increase the inside reactor vessel size to about 38 ft in diameter and about 47 ft in height.

The hexagonal fuel element assemblies are machined from graphite which acts as both the moderator for the neutrons and as structural support for the reactor. The fuel, which generates heat internally during reactor operation, consists of highly enriched uranium and fertile thorium in carbide form. It is contained in fuel holes machined in the graphite. These fuel holes, which are typically 1/2 in. in diameter, extend vertically through about 95% of the 31 in. height of the right hexagonal prism. The cooling of the fuel element assemblies is provided by the downward flow of helium at about 50 atm. pressure through coolant holes machined between the fuel holes in the graphite. A typical coolant hole diameter is 5/8 in. The center-to-center spacing between fuel holes and between fuel and coolant



holes is typically 3/4 in. In each assembly there are about 200 fuel holes and about 100 coolant holes. The cross section of a HTGR fuel element assembly is shown in Figure 1.

In each hexagonal fuel element assembly the six coolant channels in the corners of the hexagon are about 20% smaller in diameter than the other coolant channels in the assembly. Since these smaller channels amount to less than 6% of the total number, their smaller size will be neglected and the model coolant channel diameter will be selected as that of the central coolant channels. The coolant flow conditions in the model channel will be taken as those for the average channel in the reactor.

The uranium-thorium carbide fuel is coated with layers of pyrolytic carbon and bonded into rods. These rods fit into the fuel holes with about a 0.010 in. diametrical gap at room temperature. The rods span about 95% of the height of the fuel assembly element. To simplify the analysis, the model fuel rod is assumed to span the entire height of the element and the fuel rods are assumed to fit tightly into the fuel holes during reactor operation.

The model fuel rod will have a variation in power density in the axial direction. This variation will be taken as

$$q'''(Z) = q'''_0 \cos \frac{\pi Z}{H_e} \quad (1)$$

unless a computed actual axial variation is provided from another module. In Equation 1,  $q'''$  represents the thermal source strength per unit volume at any axial location  $Z$ ,  $q'''_0$  represents the thermal source strength per unit volume at the center of the fuel rod ( $Z=0$ ), and  $H_e$  is the extrapolated height of the core. Both  $q'''$  and  $q'''_0$  are taken to be constant radially

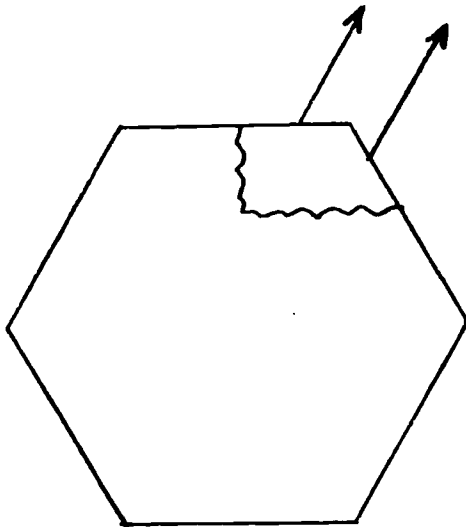
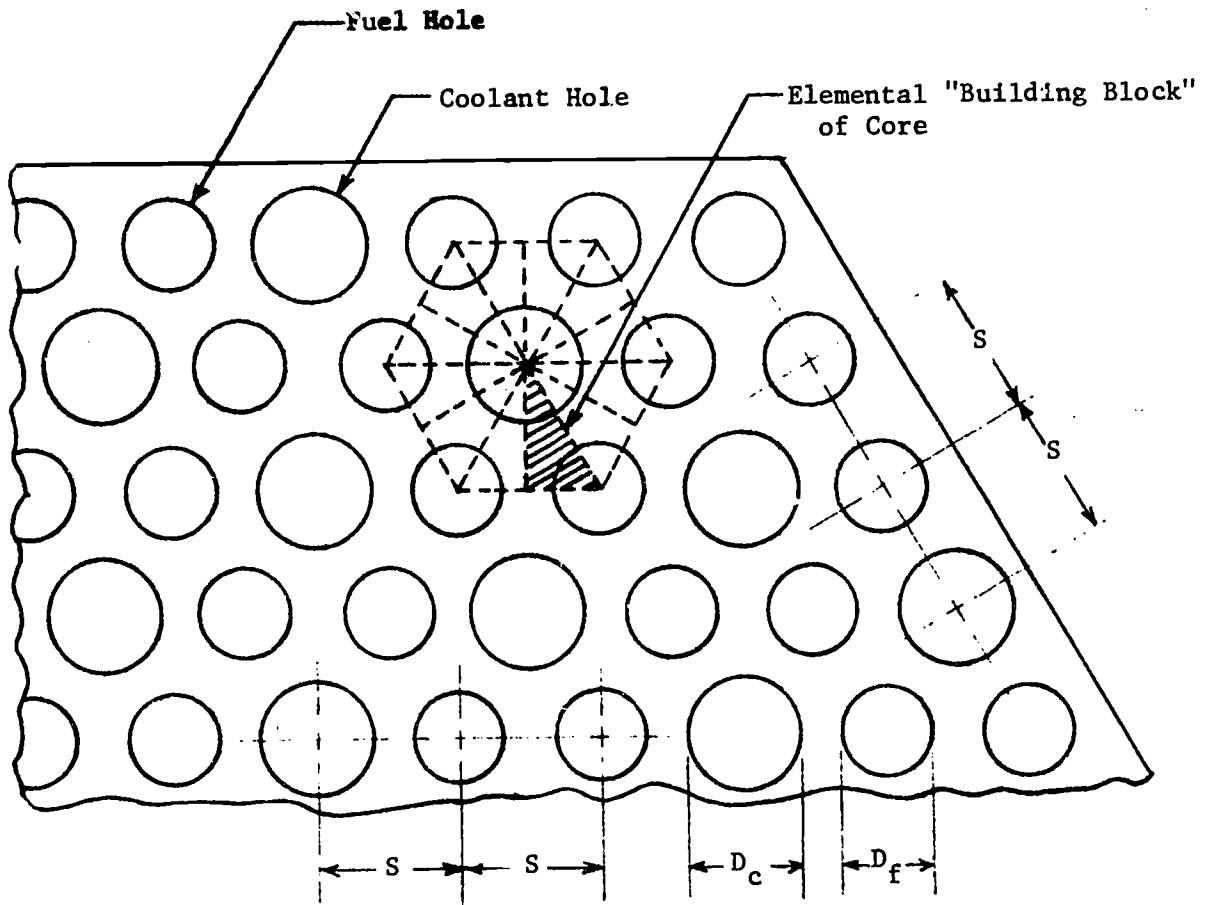


Figure 1. HTGR Fuel Geometry

throughout the fuel in the fuel rod. The magnitude of  $q''_0$  is representative of that of the average fuel rod in the core. The extrapolated height is calculated from

$$H_e = H + 2 L_e \quad (2)$$

where  $H$  is the actual height of the reactor core and  $L_e$  is an extrapolation length. The extrapolation length is the distance between the actual end of the core and the location where an extrapolation of the waveform representing the actual neutron flux distribution within the core goes to zero. From neutron diffusion theory  $L_e$  can be shown to be about one migration length for a bare core. The migration length can be calculated from neutron diffusion theory [1,2,3].\*

The triangular area shown hatched in Figure 1 represents the smallest area that can be analyzed to calculate the thermal-hydraulic behavior of the entire core. Note that all except about 1% (at the periphery of the hexagonal boundary) of the fuel element assembly can be constructed exactly from combinations of this basic "building block." The remainder can be approximated by this "building block." The segment of moderator enclosed in the triangular area will serve, in this module, as the model of the moderator for the thermal-hydraulic analysis.

The reflector regions at the inlet (top) and outlet (bottom) of the core are each about 4 ft long. Therefore, for purposes of calculating coolant pressure losses, the additional lengths of coolant channel at the inlet and outlet of the core will each be assumed equal to 20% of the core height.

---

\*Numbers in brackets refer to items in References.

#### 4.0 HTGR Thermal-Hydraulic Theory

##### 4.1 Internal Heat Generation

As a result of nuclear fission in the fuel, heat is generated. The rate of energy generation in the fuel per unit volume is called the "volumetric thermal source strength,"  $q'''$ , and can be calculated from

$$q''' = E_f N_{ff} \bar{\sigma}_f \phi \quad (3)$$

where  $E_f$  is the energy released per fission reaction (energy dimensions),  $N_{ff}$  is the fissionable fuel density (fissionable nuclei per unit volume),  $\bar{\sigma}_f$  is the effective fission microscopic cross section (dimensions of area), and  $\phi$  is the neutron flux (neutrons per unit area per unit time). Note that  $q'''$  has dimensions of energy per unit volume. The details of this calculation of volumetric thermal source strength are found in Reactor Statics Module 8.

The volumetric thermal source strength varies throughout the reactor since  $\phi$ , and perhaps  $N_{ff}$ , vary. For a cylindrical reactor, axial symmetry of the reactor fuel is generally a reasonable approximation. Therefore  $q'''$  reduces to a function of only the radius,  $R$ , and the axial position,  $Z$ . Across any single fuel rod, the change in  $q'''$  is small (due to small change in  $R$ ) and  $q'''$  can therefore be considered constant across its cross section. Thus, for any single fuel rod  $q'''$  is a function of only the axial position. Also for any small axial segment of a fuel rod (the order of 2 to 3% of the total active length) the change in  $q'''$  is moderate. Using a constant average value for any such segment thus introduces little error into the analysis. This approximation is used in this module.

The heat generation in any small segment of the fuel can be obtained by multiplying the volumetric thermal source strength by the volume of the segment. For steady state conditions this energy must be removed from the fuel. The mechanism by which this heat transfer occurs within the fuel is thermal conduction.

### Example 1

A HTGR containing 5600 fuel elements stacked 8 elements high generates 4000 Mw(t). The cylindrical core of the reactor is 21 ft long and 32 ft in diameter. Each fuel element consists of a 31.5 in. high right hexagonal prism of graphite 14.2 in. across the flats and has 132 0.620 in. diameter fuel holes each containing a tight fitting uranium-thorium fuel rod. The volumetric thermal source strength of the fuel varies as  $q''' = q'''_0 \cos(\pi Z/H_e)$ . The extrapolation length for the fuel is 1 ft. Find the average power per unit length (in kw/ft) and  $q'''_0$  for the typical 21 ft high column of fuel rods in the core.

### Solution

The power generated in the typical 21 ft high column of fuel rods is

$$P_{ave} = \frac{P_{total}}{N} = \frac{4000 \times 10^6}{(5600)(1/8)(132)} = 43,300 \text{ watt} = 43.3 \text{ kw.}$$

Thus, per unit length the average power is  $\frac{P_{ave}}{L} = \frac{43.3 \text{ kw}}{21 \text{ ft}} = 2.06 \frac{\text{kw}}{\text{ft}}$ .

The power produced by the average fuel rod column can also be calculated by integrating the power produced in each differential volume of the fuel rods. Thus,

$$P_{ave} = \int_V q''' dV = \int_{-H/2}^{H/2} q'''_0 \cos(\pi Z/H_e) (\pi D_f^2/4) dZ$$

$$\begin{aligned}
 &= (H_e D_f^2 q_o''' / 4) [\sin(\pi Z / H_e)]_{-H/2}^{H/2} \\
 &= (H_e D_f^2 q_o''' / 2) \sin(\pi H / 2H_e).
 \end{aligned}$$

Solving for  $q_o'''$ :

$$\begin{aligned}
 q_o''' &= \frac{2P_{ave}}{H_e D_f^2 \sin(\pi H / 2H_e)} \\
 &= \frac{(2)(43,300 \text{ watt})(3.413 \frac{\text{Btu}}{\text{watt-hr}})}{(23 \text{ ft})(0.62 \text{ in})^2 (\frac{1}{12} \frac{\text{ft}}{\text{in}})^2 \sin[(\pi)(21 \text{ ft}) / (2)(23 \text{ ft})]} \\
 &= 4.86 \times 10^6 \text{ Btu/hr-ft}^3.
 \end{aligned}$$

#### 4.2 Temperature Distribution in the Fuel

For conduction heat transfer the heat flux is proportional to the normal temperature gradient. When the proportionality constant is inserted,

$$q_n = -kA_n \frac{\partial T}{\partial x_n} \quad (4)$$

where  $q_n$  is the heat transfer rate in the n-direction (energy/time),  $\partial T/\partial x_n$  is the temperature gradient in the n-direction (degrees/length),  $A_n$  is the area normal to the n-direction, and  $k$  is the thermal conductivity of the material (energy/degree-length-time). Equation 4, which is Fourier's law of heat conduction, relates the heat transfer to the temperature field and is also the defining equation for the thermal conductivity. The thermal conductivity is a material property and its magnitude in general varies with the temperature of this material. Heat transfer properties of various reactor materials are tabulated as functions of temperature in References 4, 5, 6, and 7. To reduce the complexity of heat transfer calculations, the thermal conductivity is often assumed to be constant and evaluated at an average temperature. The minus sign in Equation 4 assures that the heat transfer is in the direction of decreasing temperature. Equation 4 shows that temperature gradients are required for heat transfer. In nuclear reactor applications, where there are high heat transfer rates, large temperature variations occur. One of the primary tasks of reactor thermal-hydraulic analysis is the prediction of this temperature distribution in the fuel.

The heat conduction equation in cylindrical coordinates,

$$\frac{\partial^2 T}{\partial r^2} + \frac{1}{r} \frac{\partial T}{\partial r} + \frac{1}{r^2} \frac{\partial^2 T}{\partial \theta^2} + \frac{\partial^2 T}{\partial z^2} + \frac{q'''}{k} = \frac{1}{\alpha} \frac{\partial T}{\partial t}, \quad (5)$$

and the initial and boundary conditions prescribe the temperature distribution within the fuel rod. In this relation, the thermal conductivity,  $k$ , and the thermal diffusivity,  $\alpha$ , have been assumed constant. The development of this equation is found in heat transfer texts [4, 5, 6] and several simplified cases are given as exercises for the student. For steady state conditions, the unsteady term on the right hand side of the equation is zero, and for axial symmetry, the  $\theta$  variation disappears. For HTGR applications axial symmetry in the fuel rods is a reasonable approximation and since it greatly simplifies the analysis, this assumption will be made. It may also be observed that since the length of a fuel rod is much greater than its radius, the temperature gradients in the radial direction will be much greater than the temperature gradients in the axial direction. Therefore, to a good approximation, the heat transfer in the axial direction can be neglected with respect to that in the radial direction, and the resulting temperature distribution and heat transfer reduced to a one-dimensional case for any axial segment in which  $q'''$  may be assumed constant. The governing differential equation for this case reduces to the ordinary differential equation,

$$\frac{d^2 T}{dr^2} + \frac{1}{r} \frac{dT}{dr} + \frac{q'''}{k_f} = 0. \quad (6)$$

The solution of Equation 6 subject to the boundary conditions

$$\begin{aligned} T &= T_o \text{ at } r = 0, \\ \frac{dT}{dr} &= 0 \text{ at } r = 0 \end{aligned} \quad (7)$$

yields the temperature distribution in the fuel. The second boundary condition is obtained from the observation that the temperature distri-



bution must be continuous across the center of the cylinder. Observing that both  $q'''$  and  $k$  are constant and that

$$\frac{d^2T}{dr^2} + \frac{1}{r} \frac{dT}{dr} = \frac{1}{r} \frac{d}{dr} \left( r \frac{dT}{dr} \right) \quad (8)$$

Equation 6 can be written as

$$\frac{d}{dr} \left( r \frac{dT}{dr} \right) = - \frac{q'''}{k_f} r. \quad (9)$$

Integrating twice results in

$$T = - \frac{q'''}{k_f} \frac{r^2}{4} + C_1 \ln r + C_2. \quad (10)$$

Applying the boundary conditions of Equation 7, the integration constants are

$$C_1 = 0, \quad (11)$$

$$C_2 = T_o.$$

Substituting into Equation 10 gives

$$T = T_o - \frac{q'''}{4 k_f} r^2. \quad (12)$$

This relation shows the temperature distribution in the fuel to be parabolic with maximum temperature at the center. The heat transfer rate through any cylindrical shell can be calculated from Fourier's law which takes the form

$$q_r = - k_f A_r \frac{dT}{dr} \quad (13)$$

where  $A_r = 2\pi r(\Delta L)$ ,  $\Delta L$  being the length of the cylindrical shell.

Of particular interest are the temperature and heat transfer at the surface of the fuel; i.e., at  $r = r_f = D_f/2$ . At this location,

$$T_f = T_o - \frac{q'''}{4 k_f} r_f^2, \quad (14)$$

$$\begin{aligned} q_f &= -k_f 2\pi r_f (\Delta L) \left. \frac{dT}{dr} \right|_{r = r_f} \\ &= \pi r_f^2 (\Delta L) q'''. \end{aligned} \quad (15)$$

Noting that  $\pi r_f^2 \Delta L$  is the volume of the fuel rod segment of length  $\Delta L$ , it is observed that the heat transfer out of the  $r = r_f$  cylindrical shell is indeed equal to the total energy generated as calculated from  $(q''')$  (fuel volume). For one-dimensional heat transfer all of the energy generated within the fuel must be transferred out through the surface.

### Example 2

Equation 14 relates the temperatures at the center and surface of a heat-generating cylindrical fuel rod. This equation contains the thermal conductivity of the fuel which, in general, is a function of temperature. However, the analysis leading to Equation 14 assumes the thermal conductivity to be constant. Determine the temperature at which to evaluate  $k_f$  to make the assumption of constant  $k_f$  compatible with a  $k_f$  that varies linearly with temperature.

### Solution

The method of solution is to develop an expression relating  $T_o$  and  $T_f$  which assumes  $k_f = a + bT$  and then compare this result with Equation 14. We begin with Fourier's law of heat conduction,

$$q = -k_f A_r \frac{dT}{dr}.$$

Recognizing that  $q = q'''$  (volume) and  $A_r = 2\pi r(\Delta L)$ :

$$q''' \pi r^2(\Delta L) = -k_f 2\pi r(\Delta L) \frac{dT}{dr}.$$

Simplifying, separating variables, and substituting for  $k_f$ :

$$q''' r dr = -2(a + bT) dT.$$

Integrating from  $r = 0$  to  $r = r_f$  with  $q'''$ ,  $a$ ,  $b$  constant,

$$\begin{aligned} q''' \left[ \frac{r^2}{2} \right]_0^{r_f} &= -2 \left[ aT + \frac{b}{2} T^2 \right]_{T_o}^{T_f} \\ q''' \frac{r_f^2}{4} &= -a(T_f - T_o) - \frac{b}{2} (T_f^2 - T_o^2) \\ &= \left[ a + \frac{b}{2} (T_o + T_f) \right] (T_o - T_f) \end{aligned}$$

$$T_o - T_f = \frac{q''' r_f^2}{4 \left[ a + \frac{b}{2} (T_o + T_f) \right]}.$$

Comparing this with Equation 14 written as

$$T_o - T_f = \frac{q''' r_f^2}{4 k_f}$$

we see that the relations are equivalent for

$$k_f = a + \frac{b}{2} (T_o + T_f).$$

Note that this is precisely equal to  $k_f$  evaluated at the arithmetic average fuel temperature; i.e.,  $k\left(\frac{T_o + T_f}{2}\right)$ .

Example 3

In the HTGR Thermal-Hydraulics Code an expression for the average temperature of the fuel between the  $r = r_f/2$  and  $r = r_f$  radii is required. Show that this can be expressed in terms of the fuel centerline temperature,  $T_o$ , and the fuel surface temperature,  $T_f$ , as

$$T_{f \text{ ave}} = \frac{3}{8} T_o + \frac{5}{8} T_f.$$

Solution

The average fuel temperature in any region is defined as

$$T_{f \text{ ave}} = \frac{1}{V} \int_V T \, dV.$$

Expressing the differential volume and the temperature as functions of the radius,  $r$ , (using Equation 12 for the temperature).

$$T_{f \text{ ave}} = \frac{1}{V} \int_{r_f/2}^{r_f} \left( T_o - \frac{q''' r^2}{4 k_f} \right) 2\pi r dr.$$

Noting that the volume contained between  $r_f/2$  and  $r_f$  is  $3/4 \pi r_f^2$  and integrating,

$$\begin{aligned} T_{f \text{ ave}} &= \frac{4}{3\pi r_f^2} \left[ \pi T_o r^2 - \frac{\pi q''' r^4}{8 k_f} \right]_{r_f/2}^{r_f} \\ &= \frac{4}{3\pi r_f^2} \left[ \frac{3}{4} \pi T_o r_f^2 - \frac{15\pi q''' r_f^4}{128 k_f} \right] \\ &= T_o - \frac{5 q''' r_f^2}{32 k_f}. \end{aligned}$$

But  $q'''$  can be related to  $T_o$  and  $T_f$  by Equation 14 as

$$\frac{q'' r_f^2}{4k_f} = T_o - T_f.$$

Therefore,

$$\begin{aligned} T_{f \text{ ave}} &= T_o - \frac{5}{8} (T_o - T_f) \\ &= \frac{3}{8} T_o - \frac{5}{8} T_f. \end{aligned}$$

#### 4.3 Temperature Distribution in the Graphite Moderator

In theory, the temperature distribution in the graphite moderator can be obtained by solving the steady state heat conduction equation (without internal generation) subject to the boundary conditions prescribed along the periphery of the moderator. However, the section of moderator of interest is an irregular shape as shown in Figure 1. Therefore, the bounding surfaces can not be expressed as lines of constant  $x$ ,  $y$ ,  $\theta$ ,  $r$ , or  $Z$  in either a Cartesian or cylindrical coordinate system and as a result, the boundary conditions are very difficult to apply. As a consequence, an analytical solution for the temperature distribution would be very difficult to obtain and even if obtained would be cumbersome to use. Thus, in the present module, finite-difference methods are used to determine the temperatures of interest in the moderator.

The basic finite-difference technique for determining the temperature distribution in a body consists of placing a nodal structure in the body, developing the system of algebraic equations that must be satisfied by the nodal temperatures, and solving the system of equations for the individual nodal temperatures.

The nodal structure is selected as a compromise between extreme accuracy (many nodal points) and ease of solution (few nodal points). The minimum number of nodes is restricted in the sense that there should be a nodal point at each location where the temperature is of interest. In general, nodal points are placed along the boundary of the region of interest and then at equal spacings throughout the interior. However, as we will see later, the equal spacing is not a necessity, but simply a convenience. Each nodal point serves a finite-sized segment of the body

and has a well defined nodal volume and nodal surface area. The volume of all the segments taken together must comprise the body of interest. The temperature of the entire segment is taken to be equal to its nodal temperature. One convenient way of thinking of a node is as if all the material associated with each node is shrunk to the nodal point and the nodal point is connected to all adjacent nodal points by thin rods having the correct resistance to heat transfer. A numbering scheme must be used to provide identity for the individual nodes. Using the fact that there is no heat transfer through lines of symmetry, these lines can be replaced by adiabatic boundaries and the region that must be solved greatly reduced.

The algebraic equations satisfied by the nodal temperatures can be developed in two ways. The classic way is to recognize that the heat conduction equation must hold at the nodal point and then to express the partial derivatives that appear in the heat conduction equation as their finite-difference approximation. Consider the nodal structure shown in Figure 2. It has been assumed that there are no changes in the Z-direction so that the problem reduces to a two-dimensional one. The shape of the body of interest suggested the use of the Cartesian coordinate system nodal structure that was set up. The setting of  $\Delta X = \Delta Y$  was done for convenience. The heat conduction equation that must be satisfied at every point in the body, and therefore at node 9, is

$$\frac{\partial^2 T}{\partial x^2} + \frac{\partial^2 T}{\partial y^2} + \frac{q'''}{k} = 0. \quad (16)$$

The partial derivatives in this equation are now approximated as follows:

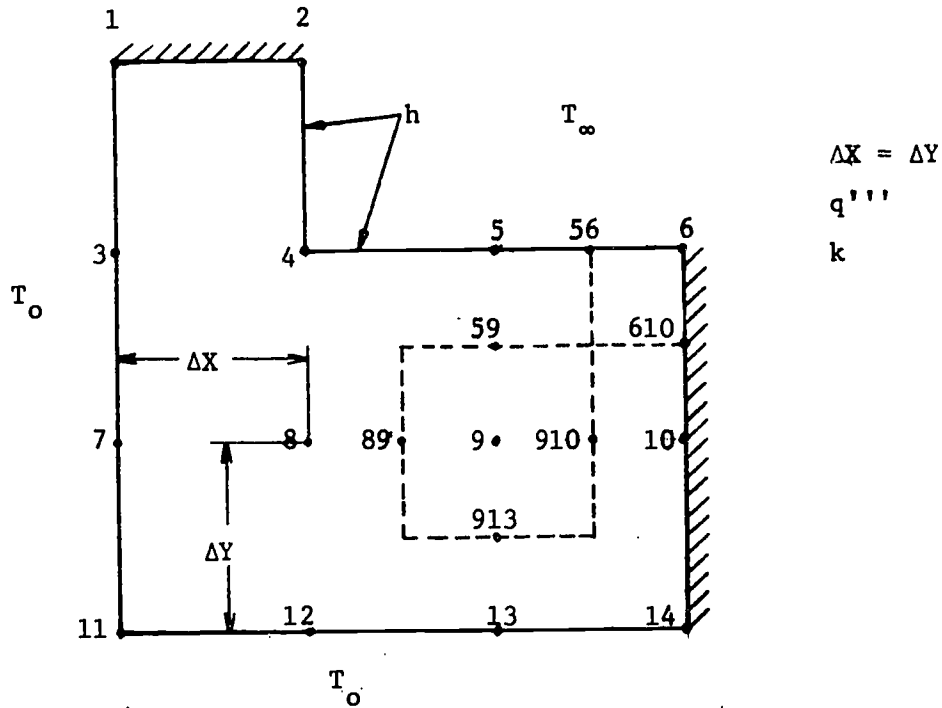


Figure 2. Finite-difference Cartesian coordinate system example

$$\left. \frac{\partial T}{\partial x} \right|_{89} = \frac{T_9 - T_8}{\Delta X}$$

$$\left. \frac{\partial T}{\partial x} \right|_{910} = \frac{T_{10} - T_9}{\Delta X}$$

$$\frac{\partial^2 T}{\partial x^2} \Big|_9 = \frac{\left. \frac{\partial T}{\partial x} \right|_{910} - \left. \frac{\partial T}{\partial x} \right|_{89}}{\Delta X} = \frac{\frac{T_{10} - T_9}{\Delta X} - \frac{T_9 - T_8}{\Delta X}}{\Delta X}$$

$$= \frac{T_{10} + T_8 - 2 T_9}{\Delta X^2}$$

(17)



$$\left. \frac{\partial T}{\partial y} \right|_{59} = \frac{T_5 - T_9}{\Delta Y}$$

$$\left. \frac{\partial T}{\partial y} \right|_{913} = \frac{T_9 - T_{13}}{\Delta Y}$$

$$\begin{aligned} \left. \frac{\partial^2 T}{\partial y^2} \right|_9 &= \frac{\left. \frac{\partial T}{\partial Y} \right|_{59} - \left. \frac{\partial T}{\partial Y} \right|_{913}}{\Delta Y} = \frac{\frac{T_5 - T_9}{\Delta Y} - \frac{T_9 - T_{13}}{\Delta Y}}{\Delta Y} \\ &= \frac{T_5 + T_{13} - 2 T_9}{\Delta Y^2} \end{aligned} \quad (18)$$

Substituting back into Equation 16,

$$\frac{T_{10} + T_8 - 2 T_9}{\Delta X^2} + \frac{T_5 + T_{13} - 2 T_9}{\Delta Y^2} + \frac{q''''}{k} = 0. \quad (19)$$

For  $\Delta X = \Delta Y$ ,

$$T_8 + T_{10} + T_5 + T_{13} - 4 T_9 + \frac{q''''(\Delta X)^2}{k} = 0. \quad (20)$$

This is the desired nodal equation for node 9. Similar equations can readily be obtained for all interior nodes of the body. The extension to boundary nodes and especially convective boundary nodes such as nodes 4 and 5 in this example is somewhat more difficult and will not be demonstrated for this method. Instead, the energy balance method, which is readily extended to all types of nodes, will be used in this module.

To show the equivalence in the methods, the nodal equation for node 9 will be determined by the energy balance method. For steady state

conditions the sum of the energy added to each nodal volume through its boundaries and the energy generated within the nodal volume must equal zero. Otherwise, there would be a net energy input to the nodal volume which violates the steady state (no changes with time) criterion. Thus, for node 9,

$$q_{8 \rightarrow 9} + q_{10 \rightarrow 9} + q_{5 \rightarrow 9} + q_{13 \rightarrow 9} + q'''(\text{nodal volume}) = 0. \quad (21)$$

Each of the boundary heat transfer rates occur by conduction and can be determined from Fourier's law,

$$q_n = -k A_n \frac{\partial T}{\partial x_n}. \quad (4)$$

Expressed in finite-difference form this becomes

$$q_n = -k A_n \frac{\Delta T}{\Delta x_n}. \quad (22)$$

Applying this to each of the four boundary heat transfer rates,

$$\begin{aligned} q_{8 \rightarrow 9} &= k(\Delta Y)(1) \frac{T_8 - T_9}{\Delta X} \\ q_{10 \rightarrow 9} &= k(\Delta Y)(1) \frac{T_{10} - T_9}{\Delta X} \\ q_{5 \rightarrow 9} &= k(\Delta X)(1) \frac{T_5 - T_9}{\Delta Y} \\ q_{13 \rightarrow 9} &= k(\Delta X)(1) \frac{T_{13} - T_9}{\Delta Y} \end{aligned} \quad (23)$$

Note that the minus sign in Fourier's law has been absorbed in the  $\Delta T$  and  $\Delta x_n$  for each term. In general, one may note that the temperature of the node of interest always occurs behind the minus sign in the temperature difference when the heat transfer rates are into the node. This obser-

vation saves much tedious chasing of minus signs in developing the nodal equations. Substituting the individual heat transfer rates into Equation 21 and noting that the nodal volume is  $(\Delta X)(\Delta Y)$  (1),

$$k\Delta Y \frac{T_8 - T_9}{\Delta X} + k\Delta Y \frac{T_{10} - T_9}{\Delta X} + k\Delta X \frac{T_5 - T_9}{\Delta Y} + k\Delta X \frac{T_{13} - T_9}{\Delta Y} + q'''(\Delta X)(\Delta Y) = 0. \quad (24)$$

For  $\Delta X = \Delta Y$  this reduces to

$$T_8 + T_{10} + T_5 + T_{13} - 4T_9 + \frac{q'''}{k} (\Delta X)^2 = 0 \quad (20)$$

which is identical to the result obtained earlier.

The energy balance method will now be applied to node 6 to demonstrate how convective and insulated boundaries are treated. For node 6,

$$q_{5 \rightarrow 6} + q_{10 \rightarrow 6} + q_{\infty \rightarrow 6} + q'''(\text{nodal volume}) = 0. \quad (25)$$

For the two conduction heat transfer rates,

$$q_{5 \rightarrow 6} = k \left( \frac{\Delta Y}{2} \right) \frac{T_5 - T_6}{\Delta X} \quad (26)$$

$$q_{10 \rightarrow 6} = k \left( \frac{\Delta X}{2} \right) \frac{T_{10} - T_6}{\Delta Y}.$$

The convective heat transfer rate can be obtained from Newton's law of cooling,

$$q = hA(T_w - T_\infty). \quad (27)$$

For heat transfer into node 6,

$$q_{\infty \rightarrow 6} = h \left( \frac{\Delta X}{2} \right) (T_\infty - T_6). \quad (28)$$

Substituting these heat transfer rates back into Equation 25 and noting

that the nodal volume is  $(\frac{\Delta X}{2})(\frac{\Delta Y}{2})(1)$ ,

$$k \frac{\Delta Y}{2} \frac{T_5 - T_6}{\Delta X} + k \frac{\Delta X}{2} \frac{T_{10} - T_6}{\Delta Y} + h \left(\frac{\Delta X}{2}\right) (T_\infty - T_6) + q'''' \left(\frac{\Delta X}{2}\right) \left(\frac{\Delta Y}{2}\right) = 0. \quad (29)$$

For  $\Delta X = \Delta Y$ ,

$$\frac{1}{2} T_5 + \frac{1}{2} T_{10} + \frac{h\Delta X}{2k} T_\infty - \left(1 + \frac{h\Delta X}{2k}\right) T_6 + \frac{q''''(\Delta X)^2}{4k} = 0. \quad (30)$$

This is the desired nodal equation for node 6. Note that the coefficient of  $T_6$  is the negative of the sum of the coefficients of the other temperatures in the nodal equation. This observation can be used either as a check or to obtain the coefficient of the temperature of the node of interest.

With the energy balance method, the nodal equations for the remainder of the nodes in the example of Figure 2 can readily be obtained. With some practice, most of the nodal equations can be written by inspection. Also, the extension of the method to three-dimensional and one-dimensional Cartesian coordinate problems should be obvious.

Unfortunately, not all problems can be readily treated with Cartesian or even cylindrical coordinate system nodal structures. The present problem of determining the temperature distribution in the graphite moderator of the HTGR is such a problem. However, the energy balance method is quite general and can be extended to different shaped nodal volumes. Tetrahedron shaped nodal volumes are convenient for general three-dimensional problems and triangular right prism nodal volumes are convenient for two-dimensional problems since most bodies can readily be decomposed into a number of these shapes. Replacing arcs with their chords permits curved surfaces to be treated with little increased

complexity and usually with acceptable accuracy. In the present moderator temperature distribution problem, temperature gradients in the vertical direction are several orders of magnitude less than those in the horizontal directions so that the problem can be treated as two-dimensional. Thus, a triangular right prism nodal structure of unit depth (triangular in the plan view) will be used.

An expression for the conduction heat transfer rates between nodes having a triangular structure must first be developed. Consider the general triangular nodal structure problem shown in Figure 3. The only

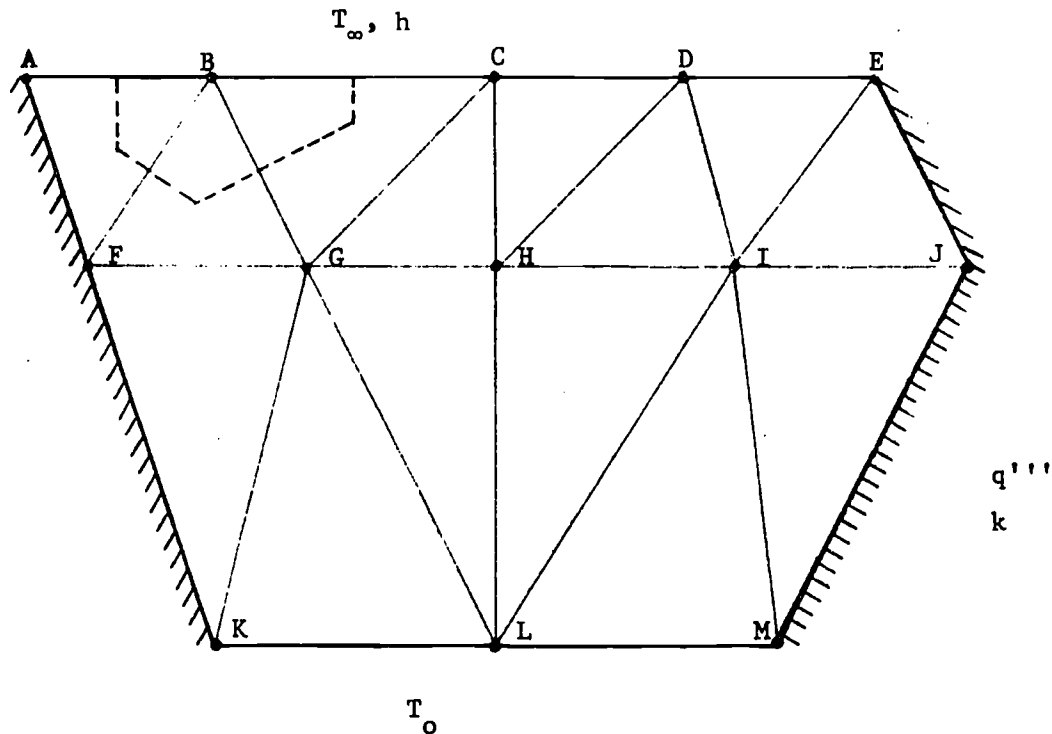


Figure 3. Triangular nodal structure example.

restriction is that all of the angles of the triangles must be less than or equal to  $90^\circ$ . The nodal equation for node B is obtained from the following energy balance for steady state conditions:

$$q_{A \rightarrow B} + q_{C \rightarrow B} + q_{F \rightarrow B} + q_{G \rightarrow B} + q_{\infty \rightarrow B} + q_{\text{gen}} = 0. \quad (31)$$

To calculate the internal energy generation for node B the nodal volume associated with node B must be defined. This nodal volume is taken as the volume (per unit depth) enclosed by the dashed lines surrounding node B. This boundary is composed of perpendicular bisectors of all the lines linking node B to the other nodes. With the nodal volume of node B,  $V_B$ , thus defined, the internally generated energy is

$$q_{\text{gen}} = q''' V_B. \quad (32)$$

The convective heat transfer rate can be calculated from Newton's law of cooling as

$$q_{\infty \rightarrow B} = h A_{\text{conv } B} (T_\infty - T_B) \quad (33)$$

where  $A_{\text{conv } B}$  is the distance between the midpoint of the link between nodes A and B to the midpoint of the link between nodes B and C times the unit depth.

To calculate the conduction heat transfer rates the concept of conduction shape factors is extremely useful. The conduction shape factor for heat transfer between nodes 1 and 2,  $S_{12}$ , is defined as

$$q_{1 \rightarrow 2} = k S_{12} (T_1 - T_2). \quad (34)$$

One sees immediately that for rectangular shaped nodal volumes the shape

factor is given by

$$S_{\text{Rect}} = A_n / (\Delta X_n) \quad (35)$$

where  $A_n$  is the heat transfer area perpendicular to the n-direction and  $\Delta X_n$  is the spacing between the nodes in the n-direction. For triangular nodes it has been shown by Dusinberre [8] that the shape factors are related to the cotangents of the opposite angle of the triangles through which the heat transfer occurs. Specifically for path BG,

$$S_{\text{BG}} = \frac{1}{2} \cot \text{BCG} + \frac{1}{2} \cot \text{BFG}. \quad (36)$$

Similarly, assuming no conduction through the fluid on the convective boundary,

$$S_{\text{BC}} = \frac{1}{2} \cot \text{BGC}. \quad (37)$$

Writing similar expressions for the remaining conduction shape factors and substituting into Equation 31,

$$\begin{aligned} k S_{\text{AB}} (T_A - T_B) + k S_{\text{BC}} (T_C - T_B) + k S_{\text{BF}} (T_F - T_B) + k S_{\text{BG}} (T_G - T_B) \\ + h A_{\text{conv B}} (T - T_B) + q''' V_B = 0 \end{aligned} \quad (38)$$

where

$$\begin{aligned} S_{\text{AB}} &= 1/2 \cot \text{BFA} \\ S_{\text{BC}} &= 1/2 \cot \text{BGC} \\ S_{\text{BF}} &= 1/2 \cot \text{BAF} + 1/2 \cot \text{BGF} \\ S_{\text{BG}} &= 1/2 \cot \text{BFG} + 1/2 \cot \text{BCG}. \end{aligned} \quad (39)$$

This relation can be simplified to

$$T_B = \frac{1}{S_B} [S_{AB}T_A + S_{BC}T_C + S_{BF}T_F + S_{BG}T_G + \frac{hA_{conv} B}{k} T_\infty + \frac{q'''V_B}{k}] \quad (40)$$

where

$$S_B = S_{AB} + S_{BC} + S_{BF} + S_{BG} + \frac{hA_{conv} B}{k}.$$

Similar expressions can be developed for each of the other nodes in the problem.

The nodal equations developed above carry an implied assumption of constant thermal conductivity. If the temperature varies significantly from node to node and the thermal conductivity is a strong function of temperature the validity of this assumption is in question. In this case, a better thermal conductivity to use in each of the heat conduction terms is the arithmetic average of the thermal conductivities evaluated at the two nodal temperatures; i.e.,

$$k_{AB} = [k(T_A) + k(T_B)]/2. \quad (41)$$

If  $k(T)$  is substituted into the nodal equations the resulting equations become nonlinear and more difficult to solve. However, often the use of a  $k$  evaluated at the average temperature of the problem suffices. Here a nodal volume weighted  $k$  would be the best value to use, but is tedious to calculate. Hence, a thermal conductivity evaluated at the arithmetic mean temperature in the problem is generally used.

The nodal equations developed as described above for constant thermal conductivity constitute a set of linear algebraic equations for the nodal temperatures. These can be readily solved by standard, well-known methods



such as matrix inversion, elimination, iteration, or relaxation. Each of these methods are well suited for computer calculations which are generally made for problems of more than a few nodes.

Equation 40 is in a form directly useable for iteration methods. In iteration schemes, the temperature distribution in the body is first assumed. (Any rough, but logical, estimate works.) Then these assumed temperatures are substituted into the right-hand side (RHS) of the equations to calculate the temperatures on the left-hand side of the equations. Then the calculated temperatures are compared with the temperatures used in the RHS. If they agree to the desired accuracy, the problem is over; if not, the calculated temperatures are used in the RHS and the process is repeated until the desired accuracy is achieved. Two standard iteration schemes exist. In Jacobi (total step) iteration, the temperature in the RHS are updated after the entire set of equations has been used. In Gauss-Seidel iteration, the temperatures in the RHS are updated as soon as new values become available (from earlier equations in the set). In general, the convergence of Gauss-Seidel iteration is somewhat faster.

#### Example 4

A HTGR fuel element assembly has a cross section as shown in Figure 1. The coolant hole diameter is  $D_c$ , the fuel diameter is  $D_f$ , and the spacing is  $S$ . At one level in the core the coolant temperature is  $T_B$ , the heat transfer coefficient is  $h$  and the volumetric thermal source strength is  $q'''$ . Assuming no heat conduction in the axial direction, set up the equations for an iterative scheme to compute the temperature distribution in the moderator.

Solution

The section of moderator that must be analyzed is the hatched area of Figure 1. An expanded view of this region with the nodal structure added is shown in Figure 4.

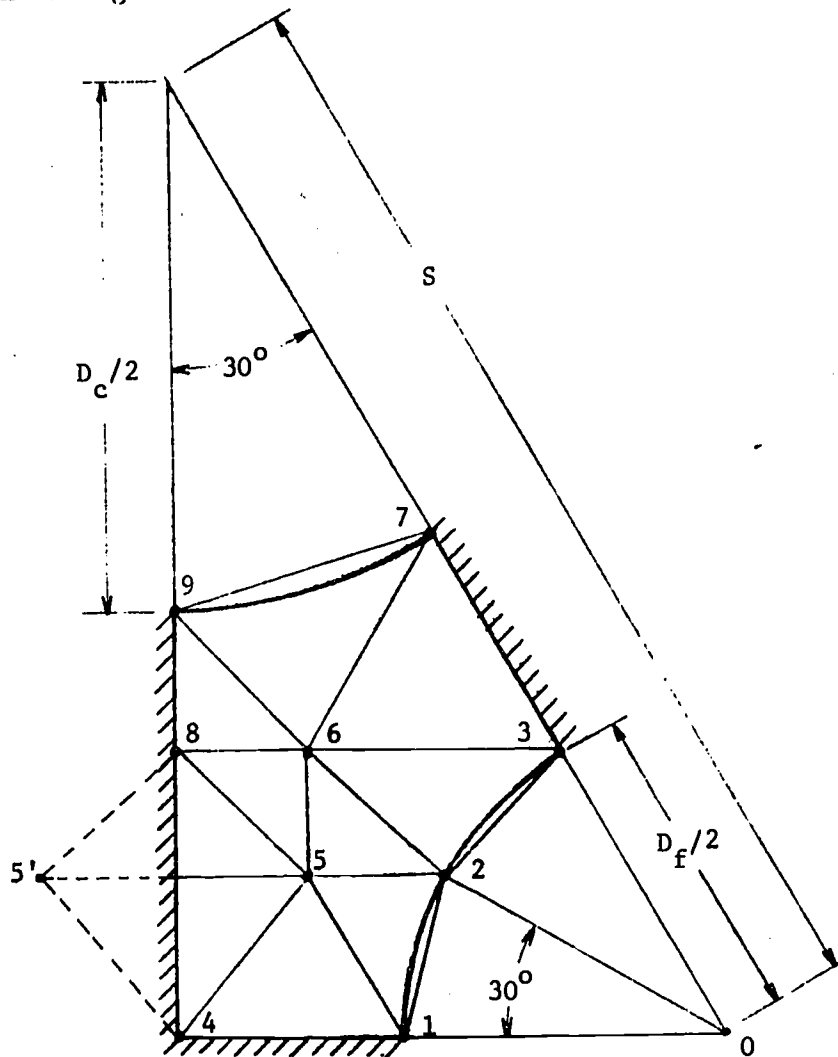


Figure 4. Geometry of Example 4 showing nodal structure.

The  $x$  and  $y$  coordinates of each of the nodal points are computed first in terms of the 3 geometric parameters,  $D_c$ ,  $D_f$ , and  $S$ .

$$\begin{aligned}
X_1 &= S \cos \frac{\pi}{3} - \frac{1}{2} D_f & Y_1 &= 0 \\
X_2 &= S \cos \frac{\pi}{3} - \frac{1}{2} D_f \cos \frac{\pi}{6} & Y_2 &= D_f \sin \frac{\pi}{6} \\
X_3 &= S \cos \frac{\pi}{3} - \frac{1}{2} D_f \cos \frac{\pi}{3} & Y_3 &= \frac{1}{2} D_f \sin \frac{\pi}{3} \\
X_4 &= 0 & Y_4 &= 0 \\
X_5 &= X_2 / 2 & Y_5 &= Y_2 \\
X_6 &= X_5 & Y_6 &= Y_3 \\
X_7 &= \frac{1}{2} D_c \sin \frac{\pi}{6} & Y_7 &= S \cos \frac{\pi}{6} - \frac{1}{2} D_c \cos \frac{\pi}{6} \\
X_8 &= 0 & Y_8 &= Y_3 \\
X_9 &= 0 & Y_9 &= S \cos \frac{\pi}{6} - \frac{1}{2} D_c
\end{aligned}$$

The conduction shape factors are determined next. The cotangents in the shape factors are expressed in terms of the nodal point coordinates calculated above.

$$\begin{aligned}
S_{12} &= \frac{1}{2} (X_1 - X_5) / Y_5 + \frac{1}{2} \frac{k_f}{k_m} \cot \frac{\pi}{6} \\
S_{14} &= \frac{1}{2} \cot [\text{Arctan } X_5 / Y_5 + \text{Arctan } (X_1 - X_5) / Y_5] \\
S_{15} &= \frac{1}{2} X_5 / Y_5 + \frac{1}{2} (X_2 - X_1) / Y_2 \\
S_{23} &= \frac{1}{2} (X_2 - X_6) / (Y_6 - Y_2) + \frac{1}{2} \frac{k_f}{k_m} \cot \frac{\pi}{6} \\
S_{25} &= \frac{1}{2} \cot [\text{Arctan } (X_2 - X_1) / Y_2 + \text{Arctan } (X_1 - X_5) / Y_5] \\
&\quad + \frac{1}{2} \cot [\text{Arctan } (X_2 - X_6) / (Y_6 - Y_2) + \text{Arctan } (X_6 - X_5) / (Y_6 - Y_5)] \\
S_{26} &= \frac{1}{2} (X_6 - X_5) / (Y_6 - Y_5) + \frac{1}{2} (X_3 - X_2) / (Y_3 - Y_2) \\
S_{36} &= \frac{1}{2} \cot [\text{Arctan } (X_7 - X_6) / (Y_7 - Y_6) + \text{Arctan } (X_3 - X_7) / (Y_7 - Y_3)] \\
&\quad + \frac{1}{2} \cot [\text{Arctan } (X_2 - X_6) / (Y_6 - Y_2) + \text{Arctan } (X_3 - X_2) / (Y_3 - Y_2)]
\end{aligned}$$

$$S_{37} = \frac{1}{2} (X_7 - X_6)/(Y_7 - Y_6)$$

$$S_{45} = \frac{1}{2} X_5/Y_5 + \frac{1}{2} (X_1 - X_5)/Y_5$$

$$S_{56} = \frac{1}{2} (X_2 - X_6)/(Y_6 - Y_2) + \frac{1}{2} X_5/(Y_8 - Y_5)$$

$$S_{58} = \frac{1}{2} (X_6 - X_5)/Y_6 - Y_5 + \frac{1}{2} X_5/(Y_8 - Y_5)$$

$$S_{67} = \frac{1}{2} \cot [\pi - \text{Arctan } X_6/(Y_9 - Y_6) - \text{Arctan } X_7/(Y_7 - Y_9)] \\ + \frac{1}{2} (X_3 - X_7)/(Y_7 - Y_3)$$

$$S_{68} = \frac{1}{2} \cot [\text{Arctan } X_5/(Y_8 - Y_5) + \text{Arctan } (X_6 - X_5)/(Y_6 - Y_5)] \\ + \frac{1}{2} (Y_9 - Y_8)/X_6$$

$$S_{69} = \frac{1}{2} \cot \left[ \frac{2\pi}{3} - \text{Arctan } (Y_7 - Y_9)/X_7 - \text{Arctan } (X_3 - X_7)/(Y_7 - Y_3) \right. \\ \left. - \text{Arctan } (X_7 - X_6)/(Y_7 - Y_6) \right]$$

$$S_{79} = \frac{1}{2} \cot [\pi - \text{Arctan } (Y_9 - Y_6)/X_6 - \text{Arctan } (Y_7 - Y_6)/(X_7 - X_6)]$$

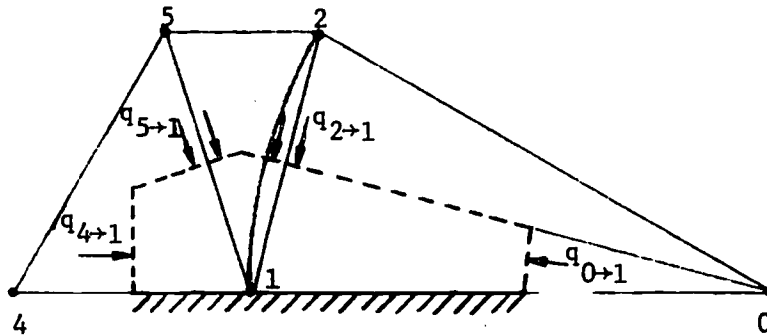
$$S_{89} = \frac{1}{2} X_6/(Y_9 - Y_6).$$

The nodal equations can now readily be developed using the above shape factors in the conduction terms. To assist in these developments, sketches of the more complex nodal volumes are useful in helping to visualize the heat transfer rates that must be taken into consideration. Use is also made of the observation that lines of symmetry can be treated as adiabatic boundaries.

Node 1:

From the sketch for node 1 on the following page,

$$q_{2 \rightarrow 1} + q_{4 \rightarrow 1} + q_{5 \rightarrow 1} + q_{0 \rightarrow 1} + q_{\text{gen}} = 0.$$



The last two terms may be combined by observing that they represent the energy generated in the entire  $15^\circ$  circular segment of the fuel. With this observation,

$$k_m S_{12}(T_2 - T_1) + k_m S_{14}(T_4 - T_1) + k_m S_{15}(T_5 - T_1) + q'''' \frac{\pi}{96} D_f^2 = 0.$$

Letting

$$S_1 = S_{12} + S_{14} + S_{15}$$

and writing the nodal equation in a form convenient for iteration,

$$T_1 = \frac{1}{S_1} (S_{12}T_2 + S_{14}T_4 + S_{15}T_5 + \frac{\pi q'''' D_f^2}{96 k_m}).$$

Node 2:

This node is similar to node 1 and its nodal equation can be written by inspection as

$$T_2 = \frac{1}{S_2} (S_{12}T_1 + S_{23}T_3 + S_{25}T_5 + S_{26}T_6 + \frac{\pi q'''' D_f^2}{48 k_m})$$

where

$$S_2 = S_{12} + S_{23} + S_{25} + S_{26}.$$

Node 3:

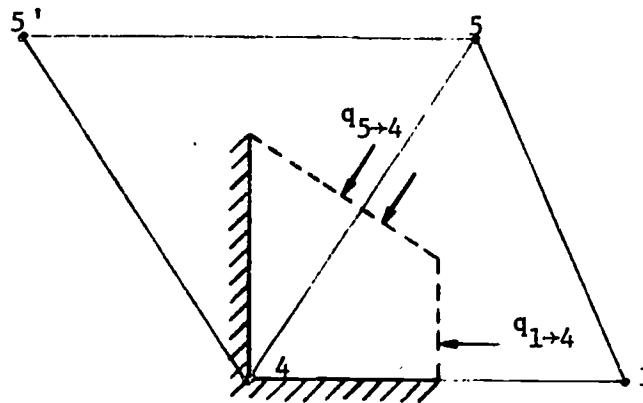
Again by inspection,

$$T_3 = \frac{1}{S_3} (S_{23}T_2 + S_{36}T_6 + S_{37}T_7 + \frac{\pi q'''' D_f^2}{96 k_m})$$

where

$$S_3 = S_{23} + S_{36} + S_{37}.$$

Node 4:



$$q_{1 \to 4} + q_{5 \to 4} = 0.$$

Note that heat transfer between nodes 4 and 8 need not be considered because there is no finite area through which this heat transfer can occur. The use of image nodes (e.g. 5') across adiabatic boundaries

helps in visualizing the problem. Solving for  $T_4$ ,

$$T_4 = \frac{1}{S_4} (S_{14}T_1 + S_{45}T_5)$$

where

$$S_4 = S_{14} + S_{45}.$$

Nodes 5, 6, and 8 are simple pure conduction nodes.

Node 5:

$$T_5 = \frac{1}{S_5} (S_{15}T_1 + S_{25}T_2 + S_{45}T_4 + S_{56}T_6 + S_{58}T_8)$$

where

$$S_5 = S_{15} + S_{25} + S_{45} + S_{58}.$$

Node 6:

$$T_6 = \frac{1}{S_6} (S_{26}T_2 + S_{36}T_3 + S_{56}T_5 + S_{67}T_7 + S_{68}T_8 + S_{69}T_9)$$

where

$$S_6 = S_{26} + S_{36} + S_{56} + S_{67} + S_{68} + S_{69}.$$

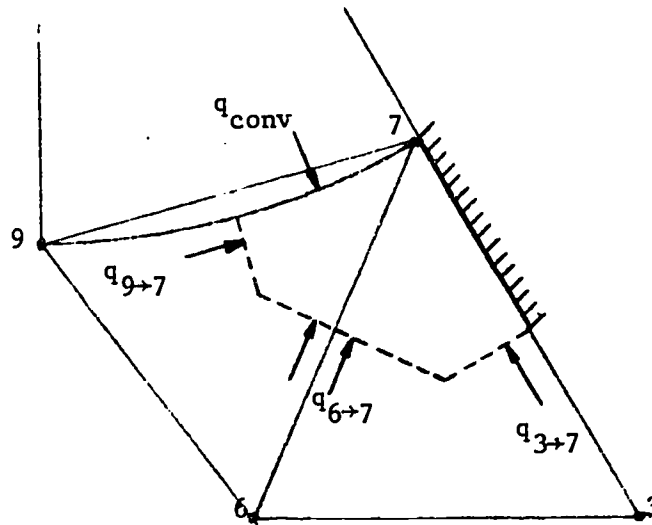
Node 8:

$$T_8 = \frac{1}{S_8} (S_{58}T_5 + S_{68}T_6 + S_{89}T_9)$$

where

$$S_8 = S_{58} + S_{68} + S_{89}.$$

Node 7:



Note that the actual circular arc heat transfer area is indicated. This will give a better representation of the heat transfer resistance in the convective layer than the chord length.

$$q_{3 \rightarrow 7} + q_{6 \rightarrow 7} + q_{9 \rightarrow 7} + q_{\text{conv}} = 0.$$

$$k_m S_{37}(T_3 - T_7) + k_m S_{67}(T_6 - T_7) + k_m S_{79}(T_9 - T_7) + h \frac{\pi D_c}{24} (T_B - T_7) = 0.$$

Solving for  $T_7$ ,

$$T_7 = \frac{1}{S_7} (S_{37}T_3 + S_{67}T_6 + S_{79}T_9 + \frac{h \pi D_c}{24 k_m} T_B)$$

where

$$S_7 = S_{37} + S_{67} + S_{79} + \frac{h \pi D_c}{24 k_m}.$$

Node 9:

$$T_9 = \frac{1}{S_9} (S_{69}T_6 + S_{79}T_7 + S_{89}T_8 + \frac{h \pi D_c}{24 k_m} T_B)$$



where

$$S_9 = S_{69} + S_{79} + S_{89} + \frac{h \pi D}{24 k_m} c .$$

This set of nine nodal equations can now be solved to determine the steady state temperatures at the nine nodal points in the moderator. This is the set of equations built into the HTGR Thermal-Hydraulics Code. In the HTGR Thermal-Hydraulics Code the equations are solved by an elimination method, rather than by iteration, to save computation time.

#### 4.4 Temperature Drop in the Convective Layer

All of the heat generated within the fuel ultimately must be transferred to the coolant. Thus, all of this energy must be transferred through the fluid layer near the surface of the moderator. This heat transfer mechanism, wherein the energy is carried away or convected from the solid surface by a fluid in motion is called convection. The heat transfer rate for convective heat transfer is related to the temperature difference between the surface and the bulk fluid, the driving potential for the heat transfer, by Newton's law of cooling,

$$q_c = h A_c (T_c - T_B). \quad (27)$$

This relation may also be taken as the defining equation for the heat transfer coefficient,  $h$ . The bulk temperature,  $T_B$ , is a mass-weighted average temperature of the fluid in the flow channel. It is formally defined by

$$T_B = \frac{\int_A \rho C_p U T \, dA}{m C_p}. \quad (42)$$

This is the temperature that a thermometer would indicate if immersed in a cup of fluid collected from the discharge of the flow channel in the given location.

Relations for calculating  $h$  from the flow characteristics and coolant properties have been developed. These will be treated in a later section of the module. For the moment, the quantity of interest is the temperature drop across the convective layer. In terms of  $h$  this can be obtained from Equation 27 as

$$T_c - T_B = \frac{q_c}{\pi D_c (\Delta L) h} \quad (43)$$

where  $D_c$  is the coolant hole diameter.

#### 4.5 Pressure Drop in the Coolant

All of the energy generated by nuclear fission in the fuel must be carried out of the reactor by the coolant which flows in the holes in the moderator. In a HTGR the coolant is gaseous helium which is force-circulated by a compressor. Enough pressure head must be provided by the compressor to overcome the pressure losses in the helium flow loop. The entire loop consists of the reactor flow channels, the heat exchangers, and connecting piping. Of interest here is the determination of the pressure loss incurred in the flow through the reactor core. Two types of pressure losses will be considered. These are the frictional pressure loss along the coolant channel and the entrance and exit permanent pressure losses.

The frictional pressure loss is a manifestation of the shear stress on the flowing fluid by the walls of the flow channel. This pressure loss is calculated from

$$\Delta P_F = f \frac{\Delta L}{D_c} \frac{\rho U_B^2}{2g_c} . \quad (44)$$

This relation may also be interpreted as the defining equation for the friction factor,  $f$ . The bulk velocity,  $U_B$ , found in Equation 44 is the velocity averaged across the flow channel. It is defined by

$$U_B = \frac{1}{A} \int_A U \, dA. \quad (45)$$

This velocity is related to the mass flow rate by

$$\dot{m} = \rho A U_B \quad (46)$$

or to the mass velocity by

$$G = \frac{\dot{m}}{A} = \rho U_B. \quad (47)$$

The value of the friction factor depends on the flow and surface conditions in the channel. The flow conditions are characterized by the Reynolds Number,

$$Re = \frac{\rho U_B D_c}{\mu}. \quad (48)$$

It is well known that for  $Re$  below a critical value the flow is laminar, and for  $Re$  above the critical value the flow is turbulent. For internal flows this critical  $Re$  is about 2000. Laminar flow may be thought of as an ordered process in which fluid layers slide over one another, being retarded only by the molecular interaction between the layers. The viscosity of the fluid quantifies the magnitude of this interaction. In laminar flow any disturbance in the fluid is damped by the viscous action. In turbulent flow there is an additional random transport mechanism operable. This mechanism may be modeled as eddies (finite sized patches of fluid which retain their characteristics for finite times) moving throughout the fluid, transporting mass, momentum, and energy by virtue of their movement. This action is quite violent and results in transport rates much greater than those by purely molecular activity in laminar flow. In turbulent flow, disturbances in the flow field grow and propagate resulting in increased turbulence levels downstream of the disturbances. Even in highly turbulent flows, there exists a layer near the solid bounding surfaces where the presence of the wall retards the penetration of eddies and therefore acts as a flow stabilizer. This

results in a laminar sublayer existing near any solid boundary. Even though this layer is very thin, much of the temperature and velocity change between wall and bulk conditions occurs in this layer. In reactor coolant channels the flow is highly turbulent with Re of the order of 100,000 and greater quite common.

The surface condition of the flow channel is characterized by the ratio of the surface roughness height to the diameter of the flow channel,  $\epsilon/D_c$ . The flow channel exhibits smooth tube behavior if the roughness height is less than the thickness of the laminar sublayer. For reactor coolant flow channels the surface conditions are controlled so that this criterion is met.

The smooth circular tube friction factor for the coolant channel can be determined from a Moody chart where  $f$  is plotted versus Re. These charts are found in most fluid mechanics texts and handbooks [7, 9, 10, 11]. An alternate method is to calculate  $f$  from a correlation in equation form. One of the most widely accepted for the turbulent flow conditions of reactor work is

$$f_{\text{circ}} = \frac{0.184}{\text{Re}^{0.2}} \quad (49)$$

This relation, like the Moody diagram, was obtained from a curve fit to experimental data in smooth circular tubes. The friction factor defined in this module is the Darcy-Weisbach friction factor. Care must be taken not to confuse this friction factor with the Fanning friction factor ( $f_{\text{Fan}} = f_{\text{D-W}}/4$ ) also found in the literature.

The permanent pressure losses at the inlet and exit are the result of increased viscous energy dissipation resulting from increased turbulent

activity. These losses may be calculated from

$$\Delta P_E = K \frac{\rho U_B^2}{2g_c} \quad (50)$$

In this relation K is the resistance coefficient for the inlet or exit geometry. The inlet may be approximated as a sudden contraction from a very large diameter to the coolant hole diameter. For this sudden contraction, the resistance coefficient is 0.5 [11]. Similarly, the exit may be approximated as a sudden expansion from  $D_c$  to a very large diameter. For this expansion, K is 1.0 [11].

#### Example 5

The HTGR described in Example 1 has an inlet coolant temperature of 600 F, an inlet coolant pressure of 701 psia, and a coolant mass velocity of  $8.3 \times 10^4$  lbm/hr-ft<sup>2</sup> through coolant holes 0.826 in. in diameter. The coolant exit temperature is 1400 F. Estimate the frictional pressure loss in the core. Neglect entrance and exit losses.

#### Solution

To obtain a one-step estimate, the coolant properties are evaluated at the average coolant temperature and pressure. The average coolant temperature is 1000 F. The average pressure will be assumed to be 700 psia. (This must be checked later.) At these conditions the helium properties required in the solution are

$$\begin{aligned} \mu &= 0.0889 \quad \text{lbm/hr-ft} \\ \rho &= \frac{P}{RT} = \frac{(700 \frac{\text{lb f}}{\text{in}^2})(144 \frac{\text{in}^2}{\text{ft}^2})}{(386 \frac{\text{ft-lb f}}{\text{lbm-R}})(1460 \text{ R})} = 0.179 \frac{\text{lbm}}{\text{ft}^3} \end{aligned}$$

The average coolant velocity is found from

$$U_B = G/\rho = (8.3 \times 10^4 \text{ lbm/hr-ft}^2) / (0.179 \text{ lbm/ft}^3) = 464,000 \text{ ft/hr} = 128.8 \frac{\text{ft}}{\text{sec}}$$

The Reynolds Number is

$$\begin{aligned} \text{Re} &= U_B D_C \rho / \mu \\ &= (464,000 \text{ ft/hr})(0.826 \text{ in.}) \left( \frac{\text{ft}}{12 \text{ in.}} \right) (0.179 \text{ lbm/ft}^3) / (0.0889 \text{ lbm/hr-ft}) \\ &= 64,300. \end{aligned}$$

Using the circular tube friction factor correlation,

$$\begin{aligned} f &= 0.184/\text{Re}^{0.2} = 0.184/(64,300)^{0.2} \\ &= 0.0201. \end{aligned}$$

From the defining equation for the friction factor,

$$\begin{aligned} \Delta P_F &= f(\Delta L/D_C) \rho U_B^2 / 2g_c \\ &= (0.0201)(21 \text{ ft}) \left( \frac{12 \text{ in.}}{\text{ft}} \right) (120 \text{ in.}/0.826 \text{ in.}) (0.179 \text{ lbm/ft}^3) \\ &\quad (464,000 \text{ ft/hr})^2 / (3600 \text{ sec/hr})^2 (2) (32.2 \text{ lbm-ft/sec}^2 - \text{lb-ft}) \\ &= 282.8 \text{ lb-ft/ft}^2 \\ &= 1.96 \text{ psi.} \end{aligned}$$

The average pressure in the core is  $701 - \frac{1.96}{2} = 700$  psia. Therefore, the assumed value of 700 psia was acceptable for the density calculation.

#### Example 6

Each coolant channel in the reactor core has the same pressure drop. If all coolant channels are not identical the flow will redistribute such that this equal pressure drop is attained. Determine the relation between average velocity in the coolant channel (or equivalently the



mass velocity) and the diameter of the channel which governs the flow distribution.

Solution

The frictional pressure drop is given by

$$\Delta P = f \frac{\Delta L}{D_c} \frac{\rho U_B^2}{2g_c}$$

Substituting for the friction factor,

$$\begin{aligned} \Delta P &= \frac{0.184}{Re^{0.2}} \frac{\Delta L}{D_c} \frac{\rho U_B^2}{2g_c} \\ &= \frac{0.184}{\left( \frac{U_B D_c \rho}{\mu} \right)^{0.2}} \frac{\Delta L}{D_c} \frac{\rho U_B^2}{2g_c} \end{aligned}$$

$$\propto U_B^{1.8} / D_c^{1.2}$$

if the same density and viscosity are assumed for each channel. For channels 1 and 2, each having equal pressure drop,

$$U_{B1}^{1.8} / D_{c1}^{1.2} = U_{B2}^{1.8} / D_{c2}^{1.2}$$

or

$$U_{B2} / U_{B1} = (D_{c2} / D_{c1})^{2/3}$$

#### 4.6 The Heat Transfer Coefficient

No direct analytical methods for predicting the heat transfer coefficient for turbulent flow in circular tubes exist. However, by the use of an analogy between heat and momentum transport, the dependence of  $h$  on the flow field characteristics, i.e., on the  $Re$  can be predicted. Then by applying the results of an heat transfer analysis for flow over a flat plate an estimate of the Prandtl number dependence can be obtained. The  $Pr$  may be interpreted as a dimensionless modulus relating the temperature field in the fluid to the flow field. For  $Pr$  of unity, similar velocity and temperature profiles exist in the fluid. Finally, the predicted expression for  $h$  is compared to empirical correlations found to fit the available experimental data.

The heat transfer across a fluid layer in laminar flow may be calculated from Fourier's law

$$q = -k A \frac{dT}{dy}, \quad (51)$$

where  $y$  is the direction normal to the fluid layer. Similarly, the shear stress in the fluid can be related to the velocity gradient by

$$\tau = \mu \frac{dU}{dy}. \quad (52)$$

which defines the viscosity coefficient  $\mu$ . These relations can be rearranged to yield

$$\frac{q}{\rho C_p A} = -\alpha \frac{dT}{dy} \quad (53)$$

and

$$\frac{\tau}{\rho} = \nu \frac{dU}{dy}. \quad (54)$$

In these relations,  $\alpha \equiv k/\rho C_p$  is the molecular diffusivity of heat and  $\nu$  is the kinematic viscosity or the molecular diffusivity of momentum. We now postulate that the eddy transport of heat and momentum present in turbulent flow can be expressed in the same form. To this end, we define the eddy diffusivity of heat,  $\epsilon_H$ , and the eddy diffusivity of momentum,  $\epsilon_M$ , as the parameters, that, when multiplied by the appropriate gradient, yield the corresponding transport rate for turbulent flow. In general,  $\epsilon_M$  and  $\epsilon_H$  vary throughout the flow field. For the combined molecular transport plus turbulent eddy transport,

$$\frac{q}{\rho C_p A} = -(\alpha + \epsilon_H) \frac{dT}{dy} \quad (55)$$

and

$$\frac{\tau}{\rho} = (\nu + \epsilon_M) \frac{dU}{dy} \quad (56)$$

We now assume that heat and momentum are transported by analogous processes and at the same rate. This requires that  $\alpha = \nu$  and  $\epsilon_H = \epsilon_M$ . Since the  $Pr = \nu/\alpha$ , the first condition is equivalent to  $Pr = 1$ . Similarly a turbulent Prandtl number may be defined as  $Pr_t = \epsilon_M/\epsilon_H$ . Therefore, the second condition is equivalent to  $Pr_t = 1$ . The basic assumption we have made also implies that both  $q$  and  $\tau$  vary in the same way across the flow field; i.e.,

$$\frac{q}{C_p A \tau} = \text{Constant} \equiv \frac{q_w}{C_p A_w \tau_w} \quad (57)$$

if the constant is expressed in terms of quantities at the surface or wall.

Dividing Equation 55 by Equation 56 and using the assumption discussed above,

$$\frac{q_w}{C_p A_w \tau_w} dU = -dT. \quad (58)$$

Integrating this expression between wall conditions and fluid bulk conditions,

$$\frac{q_w}{C_p A_w \tau_w} \int_{U_w}^{U_B} dU = - \int_{T_w}^{T_B} dT. \quad (59)$$

Using  $U_w = 0$ , this reduces to

$$\frac{q_w U_B}{C_p A_w \tau_w} = T_w - T_B. \quad (60)$$

To introduce  $h$  into this expression, Newton's law of cooling (Equation 27) is used to give

$$h = \frac{q_w}{A_w (T_w - T_B)}. \quad (61)$$

Substituting Equation 61 into Equation 60,

$$h = \frac{C_p \tau_w}{U_B}. \quad (62)$$

The shear stress at the wall can be eliminated from this expression in favor of the friction factor. To do this,  $\tau_w$  is first related to the pressure loss over the length  $\Delta L$  of the channel and then Equation 44 relating the pressure loss and the friction factor is used. Consider the fluid in a section of channel of diameter  $D$  and length  $\Delta L$ . For fully developed flow, the sum of the forces acting in the flow direction must equal zero. The forces that must be considered are the pressure force on the upstream circular face,  $\frac{\pi}{4} D^2 P$ , the pressure force on the downstream

face,  $\frac{\pi D^2}{4} (P - \Delta P)$ , and the shear force along the periphery,  $\pi D \Delta L \tau_w$ . Summing these forces with proper regard as to their direction gives

$$\frac{\pi}{4} D^2 P = \pi D \Delta L \tau_w + \frac{\pi}{4} D^2 (P - \Delta P) \quad (63)$$

or

$$\tau_w = \frac{D}{4 \Delta L} \Delta P .$$

Using Equation 44 for  $\Delta P$ , this becomes

$$\tau_w = \frac{D}{4 \Delta L} f \frac{\Delta L}{D} \frac{\rho U_B^2}{2} = f \frac{\rho U_B^2}{8} . \quad (64)$$

Substituting Equation 64 into Equation 62,

$$h = C_p \rho U_B \frac{f}{8} . \quad (65)$$

Introducing the Stanton Number, a convenient dimensionless grouping common in heat transfer work, Equation 65 becomes

$$St \equiv \frac{h}{\rho C_p U_B} = \frac{f}{8} . \quad (66)$$

Using Equation 49 for  $f$ ,

$$St = 0.023 Re^{-0.2} . \quad (67)$$

This result is often found expressed in terms of the Nusselt number defined as

$$Nu = \frac{hD}{k} . \quad (68)$$

One common interpretation of the  $Nu$  is that it is the ratio of the actual convection heat transfer from a surface to the heat transfer assuming that

only molecular conduction were present. Noting that

$$St = \frac{h}{\rho C_p U_B} = \frac{\left(\frac{hD}{k}\right)}{\left(\frac{\rho}{k}\right) \left(\frac{\mu}{\rho DU_B}\right)} = \frac{Nu}{Pr Re}, \quad (69)$$

we can rewrite Equation 67 as

$$Nu = 0.023 Pr Re^{0.8}. \quad (70)$$

The Pr dependence found in Equation 70 is not correct. One reason why this incorrect dependence appears is that  $Pr = 1$  was assumed early in the development; therefore, one would not expect the Pr dependence to be properly represented in the result. The analysis of laminar flow heat transfer from a flat plate, one of the few cases which can be treated analytically, yields a  $Pr^{1/3}$  dependence as an expression for the Nusselt number. In practice it turns out that this  $Pr^{1/3}$  dependence is reasonably accurate for the turbulent pipe flow case of interest here as well. In fact some of the empirical correlations found in the literature exhibit this  $Pr^{1/3}$  dependence in the  $Nu(Pr, Re)$  relation. However, the relation that is the best known, most widely used, and is recommended here is the Dittus-Boelter Equation [12].

$$Nu = 0.023 Re^{0.8} Pr^n. \quad (71)$$

For the fluid in the tube being heated the recommended value of  $n$  is 0.4 and for the fluid in the tube being cooled the recommended value of  $n$  is 0.3. The former case is the one found in reactor work. In Equation 71 several temperature dependent fluid properties appear ( $k, \rho, \mu, C_p$ ). These properties are to be evaluated at the average bulk temperature of the fluid for the segment of tubing of interest. The heat transfer

coefficient determined from Equation 71 is the average value around the circumference of the coolant channel.

Example 7

Determine the average heat transfer coefficient for the HTGR described in Examples 1 and 5.

Solution

The average heat transfer coefficient corresponds closely to that calculated at the average coolant conditions; i.e., 1000 F and 700 psia. Additional fluid properties required for this calculation are

$$C_p = 1.248 \text{ Btu/lbm-F,}$$

$$k = 0.167 \text{ Btu/hr-ft-F.}$$

The Prandtl number is

$$\begin{aligned} Pr &= C_p \mu / k \\ &= (1.248 \text{ Btu/lbm-F})(0.0889 \text{ lbm/hr-ft}) / 0.167 \text{ Btu/hr-ft-F} \\ &= 0.664. \end{aligned}$$

From the circular tube Nusselt number correlation,

$$\begin{aligned} Nu &= 0.023 Re^{0.8} Pr^{0.4} \\ &= 0.023 (64,300)^{0.8} (0.664)^{0.4} = 137.2. \end{aligned}$$

Calculation of  $h$  from the definition of  $Nu$  gives

$$\begin{aligned} h &= (Nu) k / D_c \\ &= (137.2)(0.167 \text{ Btu/hr-ft-F}) / (0.826 \text{ in.}) \left( \frac{\text{ft}}{12 \text{ in.}} \right) \\ &= 332.8 \text{ Btu/hr-ft-F.} \end{aligned}$$

#### 4.7 Incremental Energy Balances

As heat is transferred from the fuel to the coolant, the temperature of the coolant rises. Thus, the coolant temperature varies from a minimum at the inlet of the coolant channel to a maximum at the exit of the core. The bulk temperature at any axial position can be determined from an energy balance where the total energy added by heat transfer to the coolant is equated to the energy rise of the coolant, i.e.,

$$\dot{m}i = \dot{m}i_{in} + \int_{H/2}^Z q'_c(z) dz \quad (72)$$

where  $q'_c$  is the heat transfer rate per unit length of fuel rod. Noting that for a monatomic ideal gas  $\Delta i = \frac{C_p}{Z} \Delta T_B$ , this can be rewritten as

$$T_B = T_{in} + \frac{1}{\dot{m} C_p} \int_{H/2}^Z q'_c(z) dz. \quad (73)$$

Equation 73 can be used to determine the bulk temperature increase for any segment,  $\Delta L$ , of the coolant channel by

$$T_{B2} - T_{B1} = \frac{-1}{\dot{m} C_p} \int_{Z_c + \Delta L/2}^{Z_c - \Delta L/2} q'_c(z) dz \quad (74)$$

where  $Z_c$  is the center of the increment under consideration. Defining an average surface heat flux for the increment,  $\bar{q}''_c = \bar{q}'_c / A_c$ , the incremental bulk temperature rise becomes

$$T_{B2} - T_{B1} = \frac{\pi D_c \Delta L}{\dot{m} C_p} \bar{q}''_c. \quad (75)$$

The local surface heat flux,  $q''_c(z)$ , is related to the local volumetric thermal source strength by observing that all of the energy generated in the fuel is transferred into the coolant at the coolant-moderator surface,

$$\pi D_c dz q''_c(z) = 2 \frac{\pi}{4} D_f^2 dz q'''(z). \quad (76)$$



The factor of 2 on the right-hand side accounts for the fact that the energy generated in two fuel rods is transferred to each coolant channel.

This simplifies to

$$q_c''(z) = \frac{D_f^2}{2D_c} q''''(z). \quad (77)$$

Similarly,

$$\bar{q}_c'' = \frac{D_f^2}{2D_c} \bar{q}'''' . \quad (78)$$

### 5.0 The HTGR Thermal-Hydraulics Code

The HTGR Thermal-Hydraulics Code calculates the thermal-hydraulic performance parameters discussed in Section 4 for the HTGR model described in Section 3. The basic operational steps of the code are listed below.

1. Real  $\leftrightarrow$  integer conversions
2. Definition of statement functions
3. Accept and print input
4. Calculate geometrical parameters of reactor
5. Calculate shape factors for finite-difference equations used in moderator temperature distribution calculation
6. Determine calculation increment
7. Calculate inlet pressure loss.
8. Initialize to 1st calculation increment
9. Calculate bulk temperature rise and average temperature for 1st increment
10. Calculate average coolant properties for 1st increment
11. Calculate pressure loss, exit pressure, and average pressure for 1st increment
12. Calculate heat transfer coefficient for 1st increment
13. Calculate moderator temperature distribution for 1st increment
14. Calculate temperature distribution in fuel for 1st increment
15. Print 1st increment output
16. Repeat steps 8-15 for remaining increments
17. Calculate exit pressure loss and core exit pressure
18. Print coolant exit conditions.

The details of these specific steps requiring further explanation are found in the discussion below. A flow chart showing the calculations and logic is given in Section 5.4.

The statement functions are used for convenience in calculating property data. These statement functions are in the form of some property, either of the coolant, moderator, or fuel being the function of the corresponding temperature. All of the function forms are polynomials obtained by fitting polynomials of various degree to tabulated data. The order of these polynomials varies, having been selected to insure that it is accurate to within 2% over the range of interest of the parameter.

A detailed discussion of the input requirements is deferred until Section 5.2. For the moment it suffices to note that this input is supplied on three cards; one each for the geometry, the inlet flow conditions, and the reactor power level.

The temperature distribution in the moderator is calculated from the nodal equations developed in Example 4. As preliminary calculations, the coordinate locations of the nine nodal points and the conduction shape factors are determined from the coolant hole diameter, fuel diameter, and spacing supplied as input to the code.

In the code, the model coolant channel, fuel rod, and moderator are sliced into short segments which are stacked axially to form the proper length core. The actual length of these segments is selected as a compromise between the very short segments for which the assumption of constant properties over the section axially is accurate and the very long segment which minimizes the computer time. An increment size equal to 1/50 of the active core length is built into the code. To study the effect of

increment size, or to save computer time, this can readily be changed by altering two lines of the code.

After the increment size has been computed, the coolant conditions at the beginning of the first increment are established. The bulk temperature and mass velocity at the entrance of the first increment are set equal to the core inlet conditions provided in the input. The pressure at the entrance of the first calculation increment is obtained by subtracting the inlet pressure loss, computed from Equation 44 and Equation 50, from the pressure at the inlet of the core. In addition, counters required in the code logic are set equal to 1, denoting the first increment.

The first major calculation in the code is the determination of the bulk temperature rise for the first calculation increment. This temperature rise is calculated from Equation 75 with  $\bar{q}_c''$  determined from Equation 78. For small calculation increments, the average volumetric thermal source strength can be accurately approximated by evaluating Equation 1 at  $H/2 - \Delta L/2$ ; i.e., at the center of the increment.

The average bulk temperature,  $\bar{T}_B$ , for the increment is taken as the arithmetic average of the inlet and exit values. All coolant properties, except the density, used in the pressure drop and heat transfer coefficient calculations are assumed to be functions of temperature only and are evaluated at the average bulk temperature. The density is calculated from the ideal gas law using the average bulk temperature and the inlet pressure of the increment.

Both the friction factor and heat transfer coefficient calculations require the Reynolds number of the flow which is calculated from Equation 48. Then  $f$  and  $Nu$  are calculated from Equations 49 and 71, respectively.

Knowing  $f$ , the pressure drop for the increment is calculated from Equation 44. The heat transfer coefficient is calculated from the Nu definition, Equation 68.

The temperature distribution in the moderator is calculated next. To do this, the nine finite-difference equations developed in Example 4 are solved to yield the nine nodal temperatures. An elimination method is used in this calculation. The moderator temperature distribution calculation is complicated somewhat by the fact that both the moderator and fuel thermal conductivities which appear in the finite-difference relations are temperature dependent. Therefore, an iteration on the thermal conductivities is performed. The procedure is to assume average moderator and fuel temperatures, evaluate the thermal conductivities at these assumed temperatures from the statement functions, calculate the moderator and fuel (procedure described in next paragraph) temperature distributions and average temperatures, evaluate the thermal conductivities at these new average temperatures, and compare the new and original thermal conductivities. If the new thermal conductivities are within 2% of those used in the previous iteration, the calculated moderator temperatures are accepted. If either thermal conductivity differs by more than 2%, the calculation process is repeated until finally the 2% criterion is met. The initial assumed average moderator and fuel temperature are estimated from the results of the previous calculation increment. For the first increment, an initial guess is built into the code.

After the coolant channel and moderator calculations for the increment have been performed, the radial temperature distribution in the fuel is calculated for the increment. First, the temperature at the outer

surface of the fuel is found. This is taken as the area-weighted average of the temperatures calculated at the moderator-fuel interface in the moderator finite-difference calculation. The next step is to calculate the temperature at the center of the fuel. In this calculation axial symmetry is assumed and Equation 14 is used. In Equation 14 the thermal conductivity of the fuel appears. This property is temperature dependent and should be evaluated at the mean temperature of the fuel. However, the mean fuel temperature is dependent on the temperature rise across the fuel. Thus, an iterative-type of solution is called for. The procedure used is to evaluate  $k_{f-I}$  at  $\bar{T}_f$ , calculate  $\bar{T}_0$ , calculate  $\bar{T}_{\text{fuel mean}}$ , evaluate  $k_{f-II}$  at  $\bar{T}_{\text{fuel mean}}$ , compare  $k_{f-II}$  to  $k_{f-I}$ . If  $k_{f-II}$  is within 2% of  $k_{f-I}$ , accept value of  $\bar{T}_0$ . If  $k_{f-II}$  is not within 2% of  $k_{f-I}$ , let  $k_{f-I} = k_{f-II}$  and repeat the sequence. In this way, a fuel thermal conductivity accurate to within 2% is used. The fuel temperatures at the quarter, half, and three-quarter radii are then calculated from Equation 12.

After the calculations for the first increment are completed the results are printed out. Discussion of the output is deferred until Section 5.3. It should be noted here, however, that in the output tabulation the temperatures are reported as having occurred at the axial center of the increment. In other words, for the first increment the results are reported at  $Z = H/2 - \Delta L/2$ . After the results for the first increment have been printed out, the code increments to the next segment, and continues this process until all 50 segments have been spanned.

After the completion of the calculations and printout for the 50 segments of the core, the core exit conditions are calculated and printed.

A calculation of the exit pressure loss using Equations 44 and 50 is required. Then  $P_{ex}$  and  $T_{ex}$  are computed and printed, ending the computations.

5.1 Nomenclature

<u>Analysis Symbol</u>	<u>Code Symbol</u>	<u>Description</u>
A		Area
$A_{conv}$		Convective heat transfer area
$A_f$	AFL	Flow area of coolant channel
$A_n$		Heat transfer area normal to n-direction
$A_r$		Heat transfer area at radius r
$A_c$		Heat transfer area at surface of coolant channel
$A_w$		Surface area of wall
$C_1, C_2, C_3, C_4$		Integration constants
COMP1	CØMPA1	Last iteration value of $k_f(\bar{T}_{fo})$
COMP2	CØMPA2	Last iteration value of $k_m(\bar{T}_m)$
$C_p$	CP	Constant pressure specific heat
D		Diameter
$D_f$	DFU	Outside diameter of nuclear fuel
$D_c$	DCL	Diameter of coolant channel
$E_f$		Energy release per fission
e	ERR	Error ratio
f	F	Friction factor
$g_c$		Dimensional constant = $32.174 \frac{\text{lbm-ft}}{\text{sec}^2\text{-lbf}}$
G	GIN	Mass velocity
h	HTC	Convective heat transfer coefficient
H	H	Height of active core



<u>Analysis Symbol</u>	<u>Code Symbol</u>	<u>Description</u>
$H_e$	HE	Extrapolated height of core
$i$	ENTH	Enthalpy
$i_{in}$		Enthalpy at inlet of core
INC	INC	Increment counter in code
$k$		Thermal conductivity
$k_B$	KBC	Thermal conductivity of the coolant
$k_m$	KMØ	Thermal conductivity of moderator
$k_f$	KFU	Thermal conductivity of fuel
$k_{f-I}$	KFU1	Thermal conductivity of fuel - at pre-iteration average fuel temperature
$k_{f-II}$	KFU2	Thermal conductivity of fuel - at updated average fuel temperature
$K$		Flow resistance coefficient
$L_e$		Extrapolation length
$\Delta L$	DELL	Length increment
$\dot{m}$	MDØT	Mass flow rate
$n$		Exponent in Equation 71
$N_{ff}$		Number of fissionable fuel nuclei per unit volume
$Nu$	NU	Nusselt number
Option	ØP	Option = 1 for cosine, Option = 2 for coupled program
$P_w$	PW	Wetted perimeter
$P$	PAV	Pressure
$P_1$	P1	Pressure at beginning of increment
$P_2$	P2	Pressure at end of increment
$P_{ex}$	PEX	Core exit pressure

<u>Analysis Symbol</u>	<u>Code Symbol</u>	<u>Description</u>
$P_{in}$	PIN	Core inlet pressure
$Pr$	PR	Prandtl number
$Pr_t$		Turbulent Prandtl number
$\Delta P$		Pressure drop
$\Delta P_E$	DELPE	Exit or entrance pressure loss
$\Delta P_F$	DELPF	Frictional pressure loss
$q$		Heat transfer rate
$q_f$		Heat transfer rate at $D_f$
$q_n$		Heat transfer rate in n-direction
$q_c$		Heat transfer rate at $D_c$
$q_w$		Heat transfer rate at wall
$q_{i \rightarrow j}$		Heat transfer from node i to node j
$q''_c$		Heat flux at $D_c$
$q_{gen}$		Energy generated inside nodal volume
$q'''$	QTPAV	Volumetric thermal source strength
$q'''_o$	QTFO	Volumetric thermal source strength at center of core
$q'''_{old}$	QTPOLD	Value of $q'''$ used in previous increment
$r$		Fuel rod radial coordinate
$r_f$		Radius of fuel
$R$		Core radial coordinate; also gas constant
RAT1	RAT1	Relative error in fuel thermal conductivity between iterations
RAT2	RAT2	Relative error in moderator thermal conductivity between iterations
$Re$	RE	Reynolds number
$S$	S	Center-to-center spacing between fuel rods and coolant holes

<u>Analysis Symbol</u>	<u>Code Symbol</u>	<u>Description</u>
$S_i$	SI	Coefficient of $T_i$ in nodal equations
$S_{jk}$		Conduction shape factor between nodes j and k
St		Stanton number
T	T	Temperature
$T_o$	T0	Temperature at center of fuel rod
$T_{1/4}$	T14	Temperature in fuel at $r = 1/4 r_f$
$T_{1/2}$	T12	Temperature in fuel at $r = 1/2 r_f$
$T_{3/4}$	T34	Temperature in fuel at $r = 3/4 r_f$
$T_B$	TBAV	Coolant bulk temperature
$T_{B1}$	TB1	Bulk temperature at beginning of increment
$T_{B2}$	TB2	Bulk temperature at end of increment
$T_f$	TF	Temperature in fuel at $D_f$
$T_{fo}$	TF $\phi$ AV	Average temperature in fuel between $r_f/2$ and $r_f$
$T_{ex}$	TEX	Core exit temperature
$T_{in}$	TIN	Core inlet temperature
$T_c$	TSAV	Surface temperature inside convective layer
$T_\infty$		Free stream fluid temperature
$T_w$		Wall temperature
$\Delta T$		Temperature difference
U		Velocity
$U_B$	UB	Average velocity in flow channel
V		Volume
x		Cartesian coordinate
$x_n$		Coordinate in n-direction

<u>Analysis Symbol</u>	<u>Code Symbol</u>	<u>Description</u>
X		Cartesian coordinate of nodal point
$\Delta X$		Node spacing in x-direction
y		Coordinate normal to wall
Y		Cartesian coordinate of nodal point
$\Delta Y$		Node spacing in y-direction
Z		Axial coordinate
$Z_c$	ZC	Axial location of center of increment
$\alpha$		Thermal diffusivity
$\epsilon$		Roughness size
$\epsilon_H$		Eddy diffusivity of heat
$\epsilon_M$		Eddy diffusivity of momentum
$\theta$		Angular coordinate
$\lambda_{tr}$		Transport mean free path
$\mu$	VIS	Absolute viscosity
$\nu$		Kinematic viscosity
$\rho$	RHØ	Density
$\bar{\sigma}_f$		Average fission microscopic cross section
$\tau$		Shear stress; also time
$\tau_w$		Shear stress at wall
$\phi$		Neutron flux
superscript-		Average for calculation increment

## 5.2 Code Input

The input to the HTGR Thermal-Hydraulics Code is intentionally extremely simple. Only three cards are required; the first lists the geometrical quantities, the second lists the coolant inlet conditions, and the third lists the parameters that describe the volumetric thermal source strength distribution in the reactor.

The required input data cards are listed below. The units of each parameter and their input format are included. Sample input cards are shown in Figure 5.

### Card 1 - Geometry

$D_f$	(in.)	F 10.4
$D_c$	(in.)	F 10.4
S	(in.)	F 10.4
H	(in.)	F 10.4

### Card 2 - Coolant inlet conditions

G	(lbm/hr-ft <sup>2</sup> )	E 10.3
$T_{in}$	(F)	F 10.1
$P_{in}$	(psia)	F 10.1

### Card 3 - Power distribution

$q''_o$	(Btu/hr-ft <sup>3</sup> )	E 10.3
$H_e$	(in.)	F 10.1
Option (pure number)		I 10

On Card 3 the axial volumetric thermal source strength distribution through the core is specified. For independent operation of the code (Option = 1) a cosine distribution is built into the code and  $q''_o$  and



$H_e$  are the parameters which indicate its level and period. When the HTGR Thermal-Hydraulics Code is coupled with other codes (Option = 2) the cosine distribution is over-ridden by the actual power distribution which is supplied by the main program.

### 5.3 Code Output

Three sets of information are printed out. Each is printed under completely explicit headings such that there should be no interpretation difficulties.

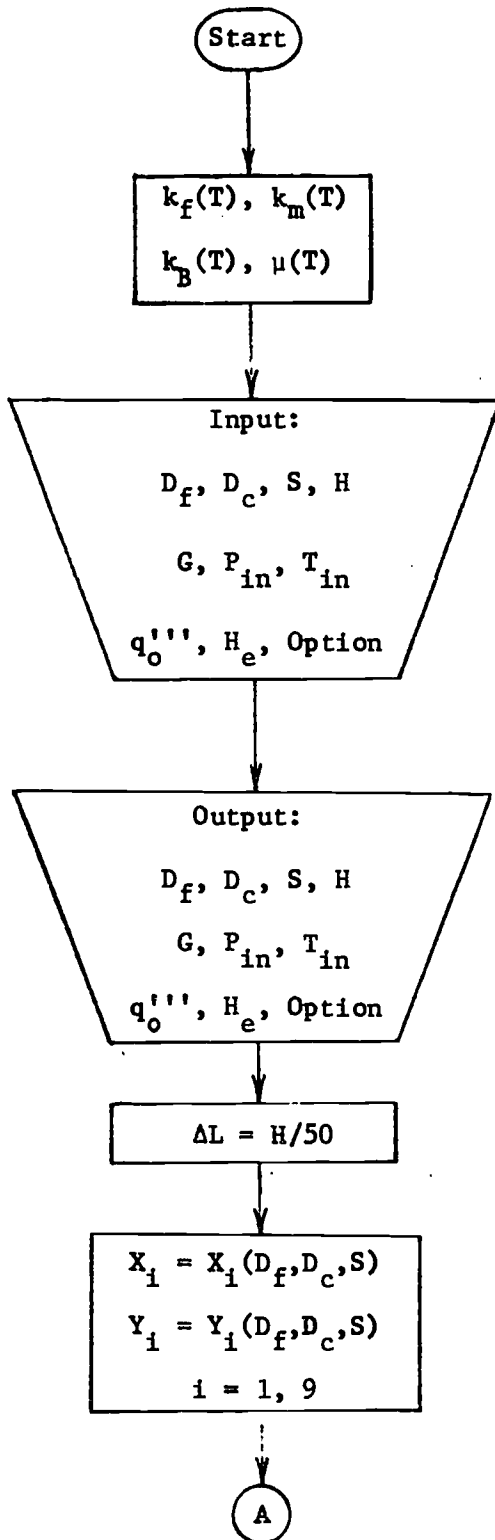
The first set of output information consists of a listing of the input that was supplied to the code.

The second and main set of output is a tabulation of the temperatures,  $h$  and  $\Delta P$  for each increment in the core. The temperature printed out are  $\bar{T}_0$ ,  $\bar{T}_{1/4}$ ,  $\bar{T}_{1/2}$ ,  $\bar{T}_{3/4}$ ,  $\bar{T}_f$ ,  $\bar{T}_B$ , and  $T_1$  through  $T_9$  in the graphite moderator. From this data, observations of the maximum fuel and moderator temperatures and their locations can be made.

The third set of data reports the core exit pressure and temperature.



## 5.4 Code Flow Chart



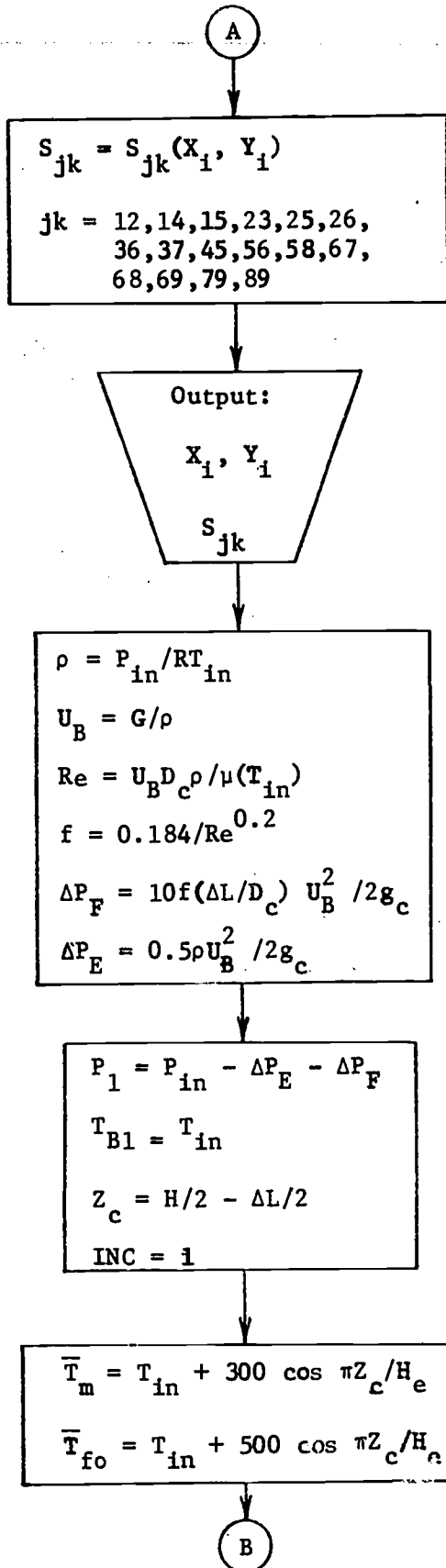
Functional relations between variables supplied to code as polynomials.

Geometry, inlet coolant conditions, and power distribution supplied to code.

Printout of geometry, inlet coolant conditions, and power distribution.

Selection of calculation increment.

Coordinates of nodal points for moderator finite-difference network are calculated.



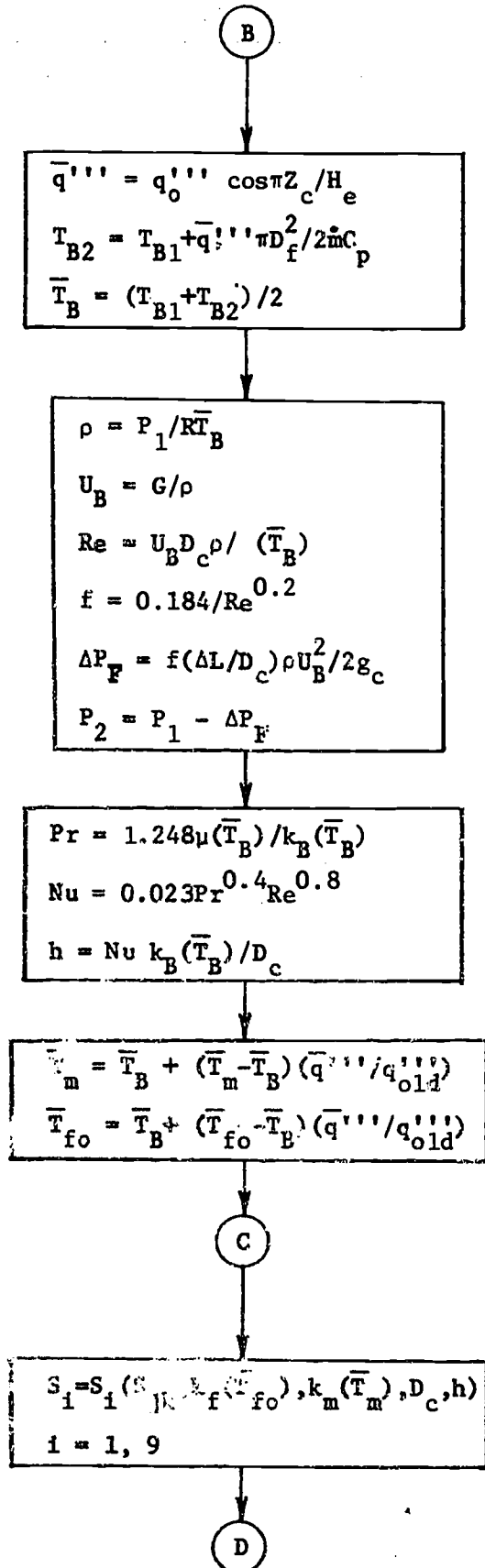
Calculation of conduction shape factors for moderator finite-difference network.

Printout of nodal point coordinates and shape factors.

Calculation of permanent pressure loss at inlet.

Initializing pressure, temperature, position, and increment counter for 1st increment.

Initial guesses for average fuel and moderator temperatures for first increment supplied to code.



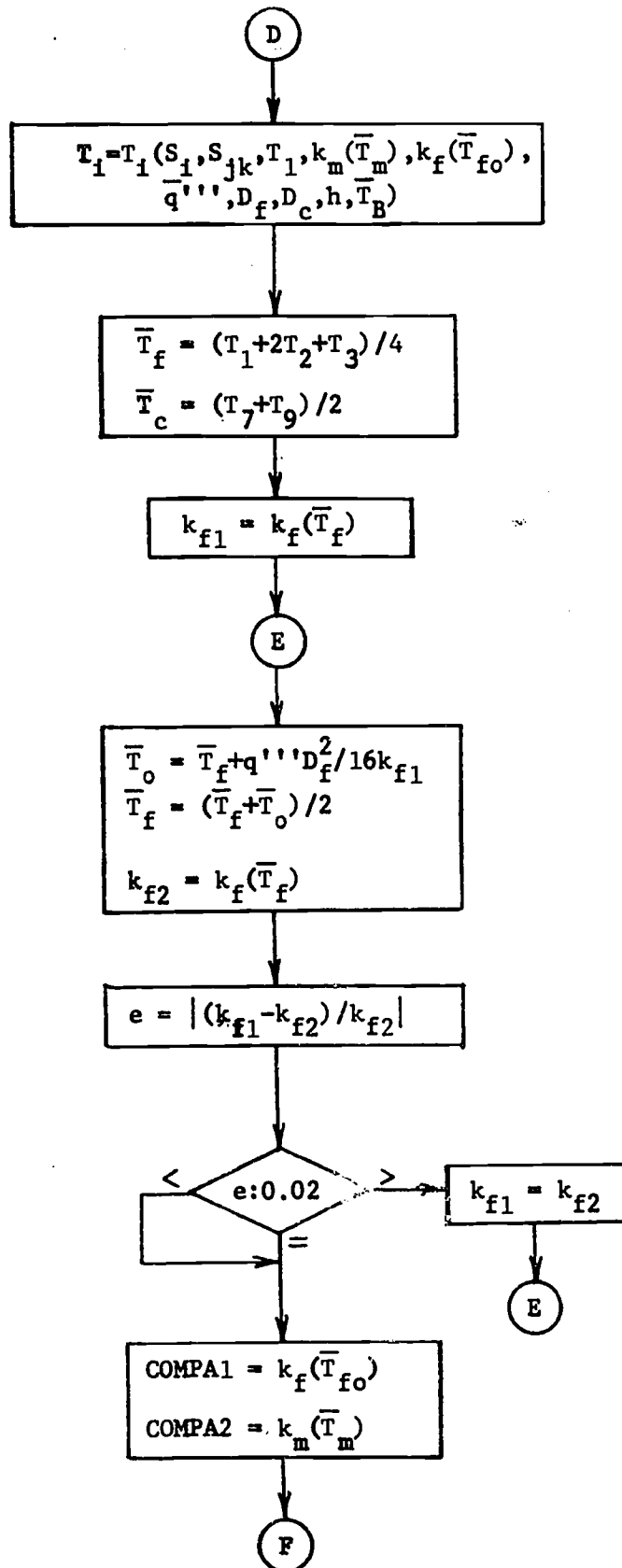
Calculation of average bulk temperature of coolant for increment.

Calculation of pressure drop and exit pressure for increment.

Calculation of average heat transfer coefficient for increment.

Obtaining best guess initial values for average fuel and moderator temperatures for finite-difference calculation.

Calculation of coefficients of  $T_i$  in nodal equations.

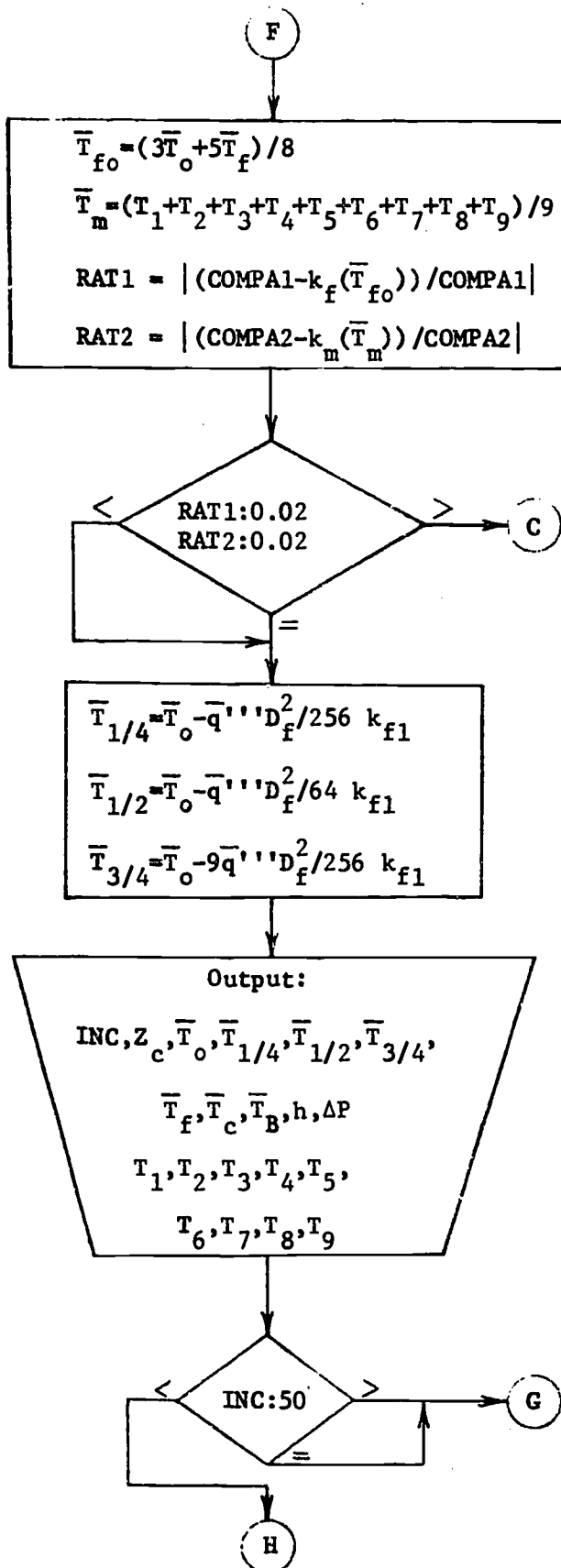


Solution of moderator temperature distribution.

Calculation of average temperatures at surfaces of fuel and coolant.

Calculation of fuel centerline temperature. The thermal conductivity of the fuel is evaluated at a mean fuel temperature by an iterative technique.

Saving values of thermal conductivities for later comparison.

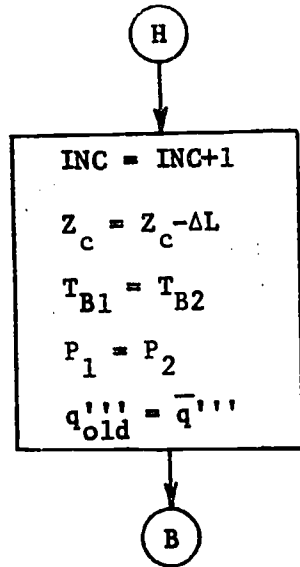


Check to determine if correct moderator and fuel thermal conductivities were used in moderator calculation. If not, an iteration on the average thermal conductivities is performed.

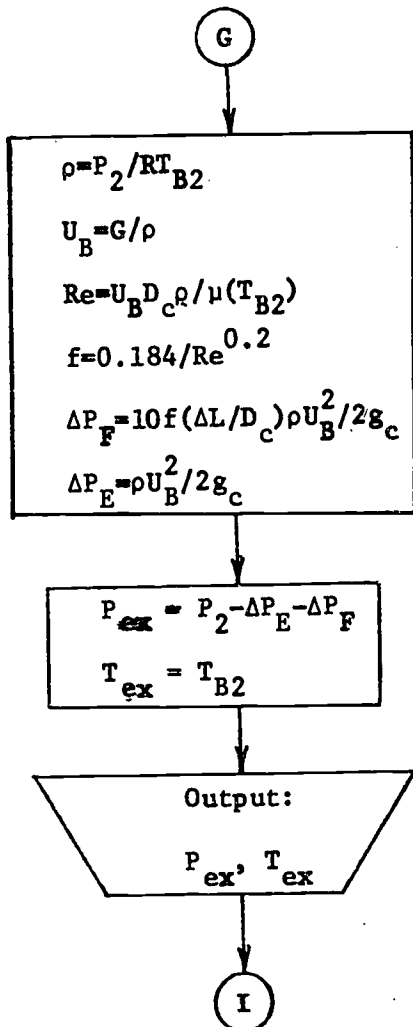
Evaluation of fuel temperature at the quarter, half, and three quarter diameter points.

Printout for increment.

Check to see if entire core has been calculated.



Initializing for next increment.



Calculation of exit pressure losses.

Calculation of coolant core exit conditions.

Printout of coolant core exit conditions.



### 5.5 Code Examples

The following two examples demonstrate the use of the HTGR Thermal-Hydraulics Code for calculating the thermal-hydraulic behavior of a typical HTGR.

#### Example 8.

A HTGR core is composed of 3000 right hexagonal prism fuel elements, each 16 in. across the flats and 32 in. high. The elements are stacked eight high in the core. The uranium-thorium fuel in carbide form fits tightly into 0.8 in. diameter fuel holes. The reactor is cooled by the downward flow of helium which enters at 500 F, 600 psia and flows through 1.0 in. diameter coolant holes. The spacing between the fuel and coolant holes is 1.25 in. The average coolant velocity in the inlet of the core is 280 ft/sec. The average fuel rod produces 4.2 kw/ft. Assume an extrapolation length equal to 5% of the core height. Determine the magnitudes and locations of the maximum fuel temperature and the maximum moderator temperature.

#### Solution.

The mass velocity, extrapolated core height, and peak volumetric thermal source strength must first be computed from the data given.

$$G = \rho_{in} U_{B in} = \frac{P_{in}}{R T_{in}} U_{B in} = \frac{(600 \frac{\text{lb}_f}{\text{in}^2})(144 \frac{\text{in}^2}{\text{ft}^2})}{(386 \frac{\text{ft-lb}_f}{\text{lbm-R}})(500 + 460) R} (280 \frac{\text{ft}}{\text{sec}}) (3600 \frac{\text{sec}}{\text{hr}})$$

$$= 2.35 \times 10^5 \text{ lbm/hr-ft}^2$$

$$H_e = H + 2L_e = H + 2(0.05H) = 1.10H$$



$$= (1.10)(8)(32 \text{ in.}) = 281.6 \text{ in.} = 23.47 \text{ ft}$$

$$\begin{aligned} q''_o &= 2P_{\text{ave}} / [H_e D_f^2 \sin(\pi H / 2 H_e)] \\ &= 2(4.2 \text{ kw/ft})(8)(32 \text{ in.}) \left( \frac{\text{ft}}{12 \text{ in.}} \right) (3413 \text{ Btu/kw-hr}) / \{ (23.47 \text{ ft})(1.0 \text{ in.})^2 \\ &\quad (\text{ft}/12 \text{ in.})^2 \sin[\pi(8)(32 \text{ in.})/2(281.6 \text{ in.})] \} \\ &= 3.79 \times 10^6 \text{ Btu/hr-ft}^3. \end{aligned}$$

From the output printout of the code (next 7 pages) we find,

$$T_{\text{mod max}} = 889.7 \text{ F at } Z = -3.63 \text{ ft at node 1}$$

$$T_{\text{fuel max}} = 962.9 \text{ F at } Z = -2.77 \text{ ft.}$$

\*\*\*\*\*  
 HTGR THERMAL-HYDRAULICS CODE  
 \*\*\*\*\*

## INPUT DATA

FUEL O.D. (INCH)	COOL O.D. (INCH)	SPACING (INCH)	ACTIVE CORE LENGTH (INCH)
0.8000	1.0000	1.2500	256.00
MASS VELOCITY (LB/HR-FT**2)	CORE INLET TEMPERATURE (F)		CORE INLET PRESSURE (PSIA)
0.2350E 06	500.00		600.00
VOLUMETRIC THERMAL SOURCE STRENGTH (BTU/HR-FT**3)	EXTRAPOLATED HEIGHT (INCH)		
0.3790E 07	281.60		

OPTION 1

END OF INPUT DATA  
 \*\*\*\*\*

## COORDINATES OF THE NODES

DFU=0.0667                      DCO=0.0833                      S=0.1042

NODE NUMBER	X COORDINATE	Y COORDINATE
1	0.18750E-01	0.00000E 00
2	0.23216E-01	0.16667E-01
3	0.35417E-01	0.28868E-01
4	0.00000E 00	0.00000E 00
5	0.11608E-01	0.16667E-01
6	0.11608E-01	0.28868E-01
7	0.20833E-01	0.54127E-01
8	0.00000E 00	0.28868E-01
9	0.00000E 00	0.48544E-01

## SHAPE FACTORS.

PATH	SHAPE FACTOR
S45	0.562500E 00
S14	0.3117972E 00
S15	0.4822120E 00
S12M	0.2142628E 00
S12F	0.8660254E 00
S25	0.1161010E 01
S26	0.4999998E 00
S23A	0.4757009E 00
S23B	0.8660254E 00
S23C	0.9514017E 00
S23D	0.4757009E 00
S29	0.2949650E 00
S28	0.1373098E 01
S36	0.4310531E 00
S27	0.4276920E 00
S29	0.3509365E 00
S37	0.1826162E 00
S79	0.4106829E 00

AT THE INLET OF THE CORE

CHANNEL AVE. VELOCITY (FT/SEC)	REYNOLDS #	FRICTION FACTOR
279.97	280285.9	0.0150

\*\*\*\*\*

NO	Z-LOC	TO	T1/4	T1/2	T3/4	TF
TN(7)	TN(1) TN(8)	TN(2) TN(9)	TN(3) TSURF	TN(4) TBULK	TN(5) HTCOF	TN(6) DELP
1	10.453	551.7	551.2	548.2	543.8	537.7
525.7	538.7 532.6	537.7 525.4	536.5 525.6	536.9 500.6	535.8 690.9	533.1 21.86
2	10.027	569.8	569.1	565.1	559.3	551.1
535.3	552.5 544.5	551.2 535.0	549.6 535.1	550.1 502.0	548.7 691.0	545.1 21.90
3	9.600	588.4	587.5	582.5	575.2	565.0
545.3	566.8 556.7	565.1 544.8	563.1 545.0	563.7 503.8	562.0 691.1	557.4 21.96
4	9.173	607.1	606.1	600.1	591.4	579.2
555.4	581.3 569.2	579.3 554.8	576.8 555.1	577.6 506.0	575.6 691.2	570.1 22.02
5	8.747	626.0	624.8	617.9	607.8	593.6
565.8	596.0 581.9	593.7 565.1	590.8 565.5	591.7 508.5	589.3 691.4	582.9 22.09
6	8.320	645.0	643.6	635.7	624.2	608.1
576.3	610.9 594.7	608.2 575.6	605.0 576.0	606.0 511.5	603.2 691.6	595.9 22.17
7	7.893	663.9	662.4	653.6	640.7	622.7
587.0	625.9 607.7	622.9 586.2	619.2 586.6	620.3 514.8	617.3 691.9	609.0 22.27
8	7.467	682.8	681.2	671.5	657.3	637.4
597.0	640.9 620.7	637.6 596.9	633.5 597.4	634.8 518.4	631.3 692.1	622.2 22.37
9	7.040	701.6	699.8	689.2	673.8	652.1
608.7	655.9 633.8	652.3 607.7	647.8 608.2	649.2 522.4	645.5 692.4	635.4 22.48
10	6.013	720.2	718.3	706.9	690.1	666.7
619.6	670.9 646.9	667.0 618.5	662.1 619.1	663.6 526.7	659.5 692.7	648.6 22.60
11	6.187	738.6	736.5	724.3	706.4	681.3
630.6	685.8 659.9	681.5 629.3	676.3 629.9	677.9 531.3	673.5 693.0	661.8 22.72

12	5.760	756.0	754.4	741.4	722.3	695.7
	700.5	690.9	690.4	692.0	687.4	674.8
	641.4	672.8	640.1	640.8	536.2	693.3
						22.36
13	5.333	774.3	771.9	758.2	738.0	709.9
	714.9	710.2	704.2	706.0	701.1	687.7
	652.3	685.6	650.8	651.5	541.4	693.7
						23.00
14	4.907	791.5	789.0	774.6	753.4	723.8
	729.2	724.1	717.9	719.8	714.5	700.4
	663.0	698.2	661.5	662.2	546.9	694.1
						23.15
15	4.480	808.1	805.6	790.5	768.4	737.5
	743.1	737.8	731.2	733.2	727.7	712.9
	673.5	710.6	672.0	672.7	552.6	694.5
						23.31
16	4.053	824.2	821.6	805.4	782.9	750.8
	750.6	751.1	744.3	746.3	740.6	725.1
	683.9	722.6	682.0	683.1	558.5	694.9
						23.47
17	3.627	839.7	836.9	820.7	796.9	763.7
	769.8	764.0	756.9	759.0	753.0	736.9
	694.1	734.4	692.4	693.2	564.7	695.3
						23.64
18	3.200	854.5	851.6	834.9	810.4	776.2
	782.5	776.5	769.1	771.3	765.1	748.4
	704.0	745.8	702.3	703.2	571.0	695.7
						23.81
19	2.773	868.5	865.6	848.4	823.3	788.1
	794.6	788.5	780.9	783.1	776.7	759.5
	713.7	756.8	711.9	712.8	577.5	696.1
						23.99
20	2.347	881.7	878.7	861.2	835.5	799.5
	806.2	799.9	792.1	794.4	787.8	770.2
	723.1	767.4	721.2	722.2	584.1	696.6
						24.17
21	1.920	894.1	891.0	873.1	847.0	810.4
	817.2	810.8	802.8	805.1	798.4	780.3
	752.1	777.4	730.2	731.2	590.9	697.0
						24.36
22	1.493	905.5	902.4	884.3	857.7	820.6
	827.5	821.0	812.9	815.2	808.4	789.9
	740.8	787.0	733.8	739.8	597.8	697.5
						24.55
23	1.067	916.0	912.9	894.5	867.7	830.1
	837.2	830.5	822.3	824.7	817.7	799.0
	749.1	796.0	747.1	748.1	604.7	697.9
						24.74

24	0.640	925.5	922.4	903.9	876.8	839.0
	846.1	839.4	831.1	833.4	826.4	807.5
756.9	804.4	754.9	755.9	611.7	698.4	24.94
25	0.213	934.0	930.8	912.3	885.1	847.1
	854.3	847.5	839.1	841.5	834.4	815.3
764.4	812.3	762.4	763.4	618.8	698.9	25.13
26	-0.213	941.4	938.3	919.7	892.5	854.5
	861.6	854.9	846.5	848.8	841.7	822.5
771.3	819.5	769.3	770.3	625.8	699.3	25.33
27	-0.640	947.8	944.6	926.1	899.0	861.0
	868.2	861.4	853.0	855.4	848.3	829.0
777.8	826.0	775.8	776.8	632.9	699.8	25.52
28	-1.067	953.0	949.9	931.5	904.5	866.8
	873.9	867.2	858.8	861.1	854.1	834.9
783.8	831.8	781.8	782.8	639.9	700.2	25.72
29	-1.493	957.1	954.0	935.8	909.0	871.7
	878.8	872.1	863.7	866.1	859.0	840.0
769.2	837.0	787.2	788.2	646.8	700.7	25.91
30	-1.920	960.1	957.0	939.0	912.6	875.7
	882.8	876.1	867.9	870.2	863.2	844.4
794.1	841.4	792.2	793.1	653.7	701.1	26.10
31	-2.347	961.9	958.9	941.2	915.2	878.9
	885.8	879.3	871.2	873.5	866.6	848.0
798.5	845.1	796.5	797.5	660.5	701.6	26.29
32	-2.773	962.5	959.6	942.2	916.8	881.2
	888.0	881.6	873.6	875.9	869.1	850.9
802.3	848.0	800.3	801.3	667.1	702.0	26.48
33	-3.200	962.0	959.2	942.2	917.4	882.6
	889.3	883.0	875.2	877.4	870.8	853.0
805.5	850.1	803.6	804.5	673.6	702.4	26.66
34	-3.627	960.4	957.6	941.1	917.0	883.2
	889.6	883.6	876.0	878.1	871.7	854.3
808.1	851.6	806.3	807.2	680.0	702.8	26.84
35	-4.053	957.6	954.9	938.9	915.5	882.8
	889.1	883.2	875.9	877.9	871.7	854.9
810.1	852.2	808.3	809.2	686.1	703.2	27.01

36	-4.430	953.7	951.0	935.7	913.1	881.6
	827.6	882.0	874.9	876.8	870.9	854.7
	811.5	852.1	809.8	810.6	692.0	703.6
37	-4.907	948.6	946.1	931.3	909.7	879.5
	885.3	879.8	873.1	874.9	869.2	853.7
	812.3	851.2	810.6	811.5	697.7	703.9
38	-5.333	942.5	940.1	926.0	905.4	876.6
	882.1	876.9	870.4	872.2	866.7	851.9
	812.5	849.6	810.9	811.7	703.2	704.3
39	-5.760	935.3	933.0	919.7	900.1	872.8
	878.0	873.1	866.9	868.6	863.4	849.4
	812.0	847.2	810.5	811.3	706.4	704.6
40	-6.187	927.1	924.9	912.3	893.9	868.1
	873.1	868.4	862.7	864.3	859.4	846.2
	811.0	844.1	809.6	810.3	713.3	704.9
41	-6.613	917.8	915.8	904.0	886.8	862.7
	867.3	863.0	857.6	859.1	854.5	842.2
	809.3	840.2	808.0	808.7	717.9	705.2
42	-7.040	907.6	905.8	894.8	878.9	856.5
	860.7	856.7	851.7	853.1	848.9	837.5
	807.1	835.7	805.9	806.5	722.2	705.4
43	-7.467	896.5	894.8	884.8	870.1	849.5
	853.4	849.7	845.2	846.4	842.6	832.1
	804.2	830.4	803.1	803.7	726.2	705.7
44	-7.893	884.5	883.0	873.9	860.5	841.8
	845.4	842.0	837.9	839.0	835.5	826.1
	800.8	824.5	799.8	800.3	729.9	705.9
45	-8.320	871.7	870.3	862.2	850.2	833.4
	836.6	833.6	829.9	831.0	827.5	819.4
	796.8	818.0	795.9	796.3	733.2	706.1
46	-8.747	858.1	856.9	849.7	839.2	824.4
	827.2	824.6	821.3	822.2	819.5	812.0
	792.2	810.8	791.4	791.8	736.1	706.3
47	-9.173	843.8	842.8	836.6	827.5	814.7
	817.1	814.9	812.1	812.9	810.5	804.1
	787.1	803.1	786.4	786.7	738.7	706.4

48	-9.600	828.8	823.0	822.8	815.1	804.5
	806.5	804.6	802.3	802.9	801.0	795.6
	781.4	794.8	780.9	781.1	740.8	706.6
						28.61
49	-10.027	813.3	812.5	808.4	802.3	793.7
	795.3	793.8	791.9	792.5	790.9	786.6
	775.3	785.9	774.8	775.0	742.6	706.7
						28.67
50	-10.453	797.1	796.6	793.4	788.8	782.4
	783.6	782.5	781.1	781.5	780.3	777.1
	768.6	776.6	768.3	768.4	744.0	706.8
						28.72

\*\*\*\*\*

EXIT PRESSURE  
(PSIA)

EXIT TEMPERATURE  
(F)

584.2

744.6

POWER PER UNIT LENGTH (KW/FT) : 2.69

\*\*\*\*\*



Example 9.

The effect of undersized coolant holes on HTGR thermal-hydraulic performance is to be studied. Consider the HTGR described in Example 8 but with a coolant hole diameter of 0.8 in. (instead of 1.0 in.). Compare the following thermal-hydraulic parameters for the "undersized coolant hole" and "normal" flow channels:

- a. Location and magnitude of maximum fuel temperature.
- b. Location and magnitude of maximum moderator temperature.
- c. Exit coolant temperature.

Solution.

Each flow channel in the core will experience the same pressure drop. The "undersized coolant hole" channel has a smaller diameter and hence will pass less flow for the same pressure loss (as shown in Example 6). To assure approximately the same pressure loss as in the "normal" channels, the mass velocity of the "undersized coolant hole" channel must be adjusted. From the results of Example 6,

$$\begin{aligned}
 G_{UCH} &= G_N (D_{UCH}/D_N)^{2/3} \\
 &= 2.35 \times 10^5 (0.8/1.0)^{2/3} \\
 &= 2.025 \times 10^5 \text{ lbm/hr-ft}^2
 \end{aligned}$$

The input to the HTGR Thermal-Hydraulics Code is the same as that for Example 8 except for the new value of  $G$  and the undersized  $D_c$ . From the code (printout next 7 pages) the following results are obtained:

- a. The maximum fuel temperature is now 1189F and occurs at  $Z = -3.63$  ft compared with 963 F at  $Z = -2.77$  ft for the "normal" channel.

\*\*\*\*\*  
 HTGR THERMAL-HYDRAULICS CODE  
 \*\*\*\*\*

## INPUT DATA

FUEL O.D. (INCH)	COOL O.D. (INCH)	SPACING (INCH)	ACTIVE CORE LENGTH (INCH)
0.8000	0.8000	1.2500	256.00
MASS VELOCITY (LB/HR-FT**2)	CORE INLET TEMPERATURE (F)		CORE INLET PRESSURE (PSIA)
0.2025E 06	500.00		600.00
VOLUMETRIC THERMAL SOURCE STRENGTH (BTU/HR-FT**3)	EXTRAPOLATED HEIGHT (INCH)		
0.3790E 07	281.60		

OPTION 1

E N D O F I N P U T D A T A  
 \*\*\*\*\*

## COORDINATES OF THE NODES

DFU=0.0667                      DCO=0.0667                      S=0.1042

NODE NUMBER	X COORDINATE	Y COORDINATE
1	0.18750E-01	0.00000E 00
2	0.23216E-01	0.16667E-01
3	0.35417E-01	0.28868E-01
4	0.00000E 00	0.00000E 00
5	0.11608E-01	0.16667E-01
6	0.11608E-01	0.28868E-01
7	0.16667E-01	0.61343E-01
8	0.00000E 00	0.28868E-01
9	0.00000E 00	0.56878E-01

## SHAPE FACTORS.

PATH	SHAPE FACTOR
S45	0.562500E 00
S14	0.3117972E 00
S15	0.4822120E 00
S12M	0.2142628E 00
S12F	0.8660254E 00
S25	0.1161010E 01
S26	0.4999598E 00
S23M	0.4757009E 00
S23F	0.8660254E 00
S56	0.9514017E 00
S58	0.4757009E 00
S89	0.2072095E 00
S68	0.1732048E 01
S36	0.6331320E 00
S67	0.3545911E 00
S69	0.2210881E 00
S37	0.7788467E-01
S79	0.8202949E 00

AT THE INLET OF THE CORE

CHANNEL AVE. VELOCITY (FT/SEC)	REYNOLDS #	FRICTION FACTOR
241.25	193218.4	0.0161

\*\*\*\*\*

NO	Z-LOC	TO	T1/4	T1/2	T3/4	TF
TN(7)	TN(1) TN(8)	TN(2) TN(9)	TN(3) TSURF	TN(4) TBULK	TN(5) HTCOF	TN(6) DELP
1	10.453	564.7	564.2	561.2	556.8	550.7
	551.7	550.7	549.5	549.8	548.8	546.0
	534.8	545.6	534.6	534.7	501.1	641.3
						21.86
2	10.027	588.3	587.6	583.6	577.8	569.6
	570.9	569.6	568.1	568.5	567.1	563.3
	548.4	562.8	548.1	548.3	503.6	641.5
						21.93
3	9.600	612.6	611.7	606.7	599.4	589.2
	590.9	589.2	587.3	587.8	586.0	581.3
	562.5	580.6	562.2	562.4	506.9	641.7
						22.02
4	9.173	637.4	636.4	630.4	621.6	609.3
	611.4	609.4	607.0	607.6	605.5	599.9
	577.2	599.0	576.8	577.0	510.8	642.0
						22.13
5	8.747	662.6	661.4	654.4	644.2	629.9
	632.4	630.0	627.3	628.0	625.5	618.9
	592.3	617.9	591.8	592.1	515.5	642.3
						22.26
6	8.320	688.2	686.8	678.9	667.3	651.0
	653.8	651.1	647.9	648.7	645.9	638.3
	607.8	637.2	607.3	607.5	520.8	642.6
						22.40
7	7.893	714.0	712.5	703.6	690.6	672.4
	675.6	672.5	669.0	669.9	666.7	658.1
	623.7	656.8	623.1	623.4	526.8	643.0
						22.57
8	7.467	740.0	738.4	728.6	714.2	694.1
	697.6	694.3	690.3	691.3	687.8	678.2
	639.9	676.7	639.2	639.5	533.4	643.4
						22.75
9	7.040	766.1	764.3	753.6	737.9	716.0
	719.9	716.2	711.8	712.9	709.0	698.5
	656.3	696.9	655.6	655.9	540.6	643.9
						22.94
10	6.613	792.2	790.3	778.7	761.8	738.1
	742.3	738.2	733.5	734.6	730.4	719.0
	672.9	717.2	672.2	672.5	548.4	644.4
						23.15
11	6.187	818.2	816.1	803.7	785.6	760.1
	764.7	760.4	755.2	756.4	751.9	739.5
	689.7	737.6	688.8	689.3	556.8	644.9
						23.38

12	5.760	844.0	841.8	828.6	309.3	782.2
	787.1	782.4	776.9	773.2	773.3	760.0
	706.5	758.0	705.6	706.1	565.7	645.5
13	5.333	869.5	867.2	853.2	832.8	804.2
	809.4	804.4	798.6	799.9	794.7	780.5
	723.4	778.3	722.4	722.9	575.1	646.0
14	4.907	894.7	892.2	877.5	856.1	826.0
	831.5	826.3	820.1	821.5	816.0	800.9
	740.3	798.6	739.3	739.8	585.0	646.7
15	4.480	919.4	916.7	901.4	879.0	847.6
	853.3	847.9	841.3	842.8	837.0	821.1
	757.0	818.6	756.0	756.5	595.4	647.3
16	4.053	943.4	940.7	924.8	901.5	868.8
	874.8	869.1	862.2	863.8	857.6	840.9
	773.7	838.4	772.6	773.1	606.1	648.0
17	3.627	966.9	964.1	947.6	923.4	889.6
	895.9	889.9	882.8	884.3	877.9	860.5
	790.1	857.8	789.0	789.5	617.3	648.6
18	3.200	989.6	986.7	969.6	944.8	909.9
	916.4	910.2	902.8	904.4	897.7	879.6
	806.4	876.8	805.2	805.8	628.7	649.3
19	2.773	1011.4	1008.4	990.9	965.4	929.6
	936.4	929.9	922.3	923.9	917.0	898.2
	822.3	895.3	821.0	821.6	640.5	650.0
20	2.347	1032.3	1029.2	1011.4	985.3	948.7
	955.6	949.0	941.1	942.8	935.7	916.2
	837.9	913.2	836.6	837.2	652.6	650.8
21	1.920	1052.2	1049.1	1030.9	1004.3	967.0
	974.1	967.4	959.2	960.9	953.6	933.7
	853.1	930.6	851.8	852.4	664.8	651.5
22	1.493	1071.0	1067.8	1049.4	1022.4	984.6
	991.8	984.9	976.6	978.3	970.8	950.4
	867.3	947.2	866.5	867.2	677.3	652.2
23	1.067	1088.6	1085.4	1066.7	1039.4	1001.2
	1008.6	1001.6	993.1	994.8	987.2	966.3
	882.1	963.1	880.8	881.4	689.9	653.0

24	0.640	1105.0	1101.8	1083.0	1055.5	1016.9
	1024.4	1017.3	1008.7	1010.4	1002.7	981.5
	895.9	978.2	894.5	895.2	702.6	653.7
						27.36
25	0.213	1120.1	1116.9	1098.0	1070.3	1031.6
	1039.2	1032.0	1023.4	1025.1	1017.2	995.8
	909.1	992.4	907.7	908.4	715.4	654.4
						27.71
26	-0.213	1133.8	1130.6	1111.7	1084.0	1045.3
	1052.9	1045.6	1036.9	1038.6	1030.7	1009.1
	921.7	1005.7	920.2	921.0	728.2	655.2
						28.06
27	-0.640	1146.1	1142.9	1124.0	1096.4	1057.8
	1065.5	1058.2	1049.4	1051.1	1043.2	1021.5
	933.6	1018.1	932.2	932.9	741.0	655.9
						28.42
28	-1.067	1156.9	1153.7	1135.0	1107.5	1069.1
	1076.8	1069.5	1060.8	1062.4	1054.5	1032.8
	944.8	1029.4	943.4	944.1	753.7	656.6
						28.77
29	-1.493	1166.3	1163.1	1144.5	1117.3	1079.3
	1086.9	1079.6	1071.0	1072.6	1064.7	1043.0
	955.4	1039.6	953.9	954.7	766.3	657.3
						29.12
30	-1.920	1174.0	1170.9	1152.6	1125.7	1088.1
	1095.7	1088.5	1079.9	1081.5	1073.7	1052.1
	965.1	1048.8	963.7	964.4	778.7	658.0
						29.47
31	-2.347	1180.2	1177.2	1159.1	1132.7	1095.7
	1103.2	1096.1	1087.6	1089.2	1081.4	1060.2
	974.1	1056.8	972.7	973.4	791.0	658.7
						29.81
32	-2.773	1184.8	1181.8	1164.1	1138.2	1102.0
	1109.3	1102.3	1094.0	1095.5	1087.9	1067.0
	982.3	1063.7	980.9	981.6	803.1	659.4
						30.15
33	-3.200	1187.8	1184.8	1167.6	1142.3	1106.9
	1114.1	1107.3	1099.1	1100.6	1093.1	1072.6
	989.5	1069.4	988.3	989.0	814.8	660.0
						30.48
34	-3.627	1189.2	1186.3	1169.5	1144.9	1110.5
	1117.5	1110.9	1102.9	1104.3	1097.0	1077.1
	996.1	1073.9	994.8	995.5	826.3	660.6
						30.81
35	-4.053	1188.9	1186.1	1169.9	1146.1	1112.8
	1119.5	1113.1	1105.3	1106.7	1099.7	1080.3
	1001.7	1077.2	1000.4	1001.1	837.5	661.2
						31.12

36	-4.480	1187.0	1184.4	1168.7	1145.7	1113.6
	1120.2	1113.9	1106.5	1107.8	1101.0	1082.3
1006.4	1079.3	1005.2	1005.8	848.2	661.8	31.43
37	-4.907	1183.6	1181.0	1166.0	1143.9	1113.1
	1119.4	1113.4	1106.3	1107.6	1101.0	1083.0
1010.2	1080.2	1009.0	1009.6	858.6	662.3	31.73
38	-5.333	1178.5	1176.1	1161.7	1140.7	1111.3
	1117.3	1111.6	1104.8	1106.0	1099.8	1082.6
1015.1	1079.9	1012.0	1012.5	868.5	662.9	32.01
39	-5.750	1171.9	1169.6	1156.0	1136.1	1108.2
	1113.8	1108.4	1102.0	1103.1	1097.2	1080.9
1015.0	1078.4	1013.9	1014.5	877.9	663.4	32.28
40	-6.187	1163.8	1161.6	1148.8	1130.0	1103.7
	1109.1	1104.0	1097.9	1099.0	1093.4	1078.1
1016.0	1075.7	1015.0	1015.5	886.8	663.8	32.54
41	-6.613	1154.3	1152.2	1140.2	1122.6	1098.0
	1103.0	1098.2	1092.5	1093.6	1088.3	1074.0
1016.1	1071.8	1015.1	1015.6	895.2	664.3	32.78
42	-7.040	1143.2	1141.3	1130.2	1113.9	1091.0
	1095.7	1091.3	1086.0	1086.9	1082.1	1068.8
1015.2	1066.8	1014.3	1014.7	903.0	664.7	33.01
43	-7.467	1130.9	1129.1	1118.9	1103.9	1082.9
	1087.1	1083.1	1078.2	1079.1	1074.7	1062.5
1013.3	1060.6	1012.5	1012.9	910.2	665.0	33.22
44	-7.893	1117.2	1115.6	1106.3	1092.6	1073.5
	1077.4	1073.7	1069.3	1070.1	1066.1	1055.1
1010.6	1053.4	1009.8	1010.2	916.8	665.4	33.42
45	-8.320	1102.2	1100.8	1092.4	1080.2	1063.1
	1066.5	1063.3	1059.3	1060.1	1056.5	1046.6
1006.9	1045.1	1006.2	1006.5	922.8	665.7	33.59
46	-8.747	1086.1	1084.8	1077.5	1066.7	1051.6
	1054.6	1051.7	1048.3	1048.9	1045.8	1037.2
1002.3	1035.8	1001.7	1002.0	928.1	666.0	33.75
47	-9.173	1068.8	1067.7	1061.4	1052.1	1039.1
	1041.7	1039.2	1036.2	1036.8	1034.1	1026.7
996.7	1025.5	996.2	996.5	932.7	666.2	33.90

Q



48	-9.600	1050.5	1049.6	1044.3	1036.5	1025.6
	1027.7	1025.7	1023.2	1023.7	1021.4	1015.3
	990.3	1014.3	989.9	990.1	936.7	666.4
						34.02
49	-10.027	1031.2	1030.5	1026.2	1019.9	1011.2
	1012.9	1011.3	1009.3	1009.7	1007.9	1003.0
	983.1	1002.2	982.7	982.9	939.9	666.6
						34.12
50	-10.453	1011.0	1010.5	1007.2	1002.5	996.0
	997.2	996.0	994.5	994.8	993.5	989.8
	974.9	989.2	974.7	974.8	942.5	666.7
						34.21

\*\*\*\*\*

EXIT PRESSURE  
(PSIA)

EXIT TEMPERATURE  
(F)

583.5

943.6

POWER PER UNIT LENGTH (KW/FT) : 2.69

\*\*\*\*\*

- b. The maximum moderator temperature is now 1120F and occurs at node 1 at  $Z = -4.48\text{ft}$  compared with 890 F for node 1 at  $Z = -3.63\text{ft}$  for the "normal" channel.
- c. The helium exit temperature is now 944F compared to 745 F for the "normal" channel.

5.6 Listing of Code

C  
C  
C-----VPI HTGR THERMAL-HYDRAULICS CODE.  
C  
C  
C

INTEGER UP  
REAL KFU,KMO,KBC,NU,MDOT,KFU1,KFU2  
DIMENSION T(9),A(81),B(9)

TEMPERATURE DEPENDENT PROPERTIES.

KFU(T)=0.15488E+02-0.72135E-02\*T+0.46776E-05\*T\*\*2-3.10256E-08\*  
< T\*\*3  
KMO(T)=0.53309E+02-0.31556E-01\*T+0.6629E-05\*T\*\*2  
KBC(T)=0.811425E-01+0.100714E-03\*T-0.142851E-07\*T\*\*2  
VIS(T)=0.40903E-01+0.6274E-04\*T-0.96155E-08\*T\*\*2

READING INPUT DATA.

READ(5,5)DFU,DCO,S,H  
5 FORMAT(3F10.4,F10.1)  
READ(5,10)GIN,TIN,PIN  
10 FORMAT(E10.3,2F10.1)  
READ(5,15)QTPO,HE,OP  
15 FORMAT(E10.3,F10.1,I10)

PRINTOUT OF INPUT DATA.

WRITE(6,20)  
20 FORMAT(1H1,2X////////15X,'\*\*\*\*\*'/15X,  
<'HTGR THERMAL-HYDRAULICS CODE'/15X,'\*\*\*\*\*'

```

<'//15X,'INPUT DATA'//)
WRITE(6,25) DFU,DCO,S,H
25 FORMAT(15X,'FUEL D.D.',6X,'COOL C.D.',7X,'SPACING',7X,'ACTIVE CORE
< LENGTH',6X,/15X,'(INCH)',9X,'(INCH)',9X,
<' (INCH)',14X,' (INCH)',14X/15X,F6.4,9X,F6.4,9X,F6.4,
<14X,F6.2,16X/)
WRITE(6,30)GIN,TIN,PIN
30 FORMAT(15X,'MASS VELOCITY',6X,'CORE INLET TEMPERATURE',3X,
<'CORE INLET PRESSURE'/15X,'(LB/HR-FT**2)',13X,' (F)',20X,'(PSIA)'/
<15X,E11.4,14X,F7.2,17X,F7.2/)
WRITE(6,35)QTPO,HE
35 FORMAT(15X,'VOLUMETRIC THERMAL',4X,'EXTRAPOLATED HEIGHT'/15X,'SOUR
<CE STRENGTH'/15X,'(BTU/HR-FT**3)',11X,'(INCH)'/15X,E11.4,14X,
<F6.2//)
WRITE(6,40)OP
40 FORMAT(19X,'OPTION',3X,I2//15X,'E N D O F I N P U T D A T A ',/
<15X,'*****',//))

```

C  
C  
C

CONVERTING INCHES TO FEET.

```

DFU=DFU/12.0
S=S/12.0
DCO=DCO/12.0
H=H/12.0
HE=HE/12.0

```

C  
C  
C  
C  
C  
C  
C

A SYSTEM OF NODES IS SET UP FOR THE FINITE-DIFFERENCE ANALYSIS OF HEAT TRANSFER IN THE GRAPHITE. THE ORIGIN OF THIS SYSTEM, THE CENTER OF THE FUEL, AND THE CENTER OF THE COOLANT HOLE FORM A RIGHT-ANGLED TRIANGLE. THE 'X', AND 'Y' COORDINATES OF THE NODES ARE CALCULATED IN TERMS OF S, THE SPACING, DFU, THE DIAMETER OF THE FUEL, AND DCO, THE DIAMETER OF THE COOLANT HOLE

C AS FOLLOWS:  
C

PI=ARCCOS(-1.0)  
X1=S\*COS(PI/3.0)-0.5\*DFU  
Y1=0.0  
X2=S\*COS(PI/3.0)-0.5\*DFU\*COS(PI/6.0)  
Y2=0.5\*DFU\*SIN(PI/6.0)  
X3=S\*COS(PI/3.0)-0.5\*DFU\*COS(PI/3.0)  
Y3=0.5\*DFU\*SIN(PI/3.0)  
X4=0.0  
Y4=0.0  
X5=X2/2.0  
Y5=Y2  
X6=X5  
Y6=Y3  
X7=0.5\*DCC\*SIN(PI/6.0)  
Y7=S\*COS(PI/6.0)-0.5\*DCO\*COS(PI/6.0)  
X8=0.0  
Y8=Y3  
X9=0.0  
Y9=S\*COS(PI/6.0)-0.5\*DCO

C  
C THE FOLLOWING SEGMENT CALCULATES THE CONDUCTION SHAPE FACTORS  
C ASSOCIATED WITH THE HEAT TRANSFER BETWEEN THE NODES. EACH SHAPE  
C FACTOR CORRESPONDS TO HALF THE SUM OF THE COTANGENTS OF THE  
C ANGLES ENCLOSING THE PATHS.  
C

S45=0.5\*(X5/Y5+(X1-X5)/Y5)  
S14=0.5\*(COTAN(ATAN(X5/Y5)+ATAN((X1-X5)/Y5)))  
S15=0.5\*(X5/Y5+(X2-X1)/Y2)  
S12M=0.5\*(X1-X5)/Y5  
S12F=0.5\*COTAN(PI/6.0)

```

S25=0.5*(COTAN(ATAN((X2-X1)/Y2)+ATAN((X1-X5)/Y5))+COTAN(ATAN((X2
< -X6)/(Y6-Y2))+ATAN((X6-X5)/(Y6-Y5))))
S26=0.5*((X6-X5)/(Y6-Y5)+(X3-X2)/(Y3-Y2))
S23M=0.5*((X2-X6)/(Y6-Y2))
S23F=0.5*COTAN(PI/6.0)
S56=0.5*((X2-X6)/(Y6-Y2)+X5/(Y8-Y5))
S58=0.5*((X6-X5)/(Y6-Y5)+X5/(Y8-Y5))
S89=0.5*X6/(Y9-Y6)
S68=0.5*((Y9-Y8)/X6+COTAN(ATAN(X5/(Y8-Y5))+ATAN((X6-X5)/
< (Y6-Y5))))
S36=0.5*(COTAN(ATAN((X7-X6)/(Y7-Y6))+ATAN((X3-X7)/(Y7-Y3)))+
< COTAN(ATAN((X2-X6)/(Y6-Y2))+ATAN((X3-X2)/(Y3-Y2))))
S67=0.5*(COTAN(PI-ATAN(X6/(Y9-Y6))-ATAN(X7/(Y7-Y9)))+(X3-X7)/
< (Y7-Y3))
S69=0.5*COTAN(PI-PI/3.0-ATAN((Y7-Y9)/X7)-ATAN((X3-X7)/(Y7-Y3))-
< ATAN((X7-X6)/(Y7-Y6)))
S37=0.5*(X7-X6)/(Y7-Y6)
S79=0.5*COTAN(PI-ATAN((Y9-Y6)/X6)-ATAN((Y7-Y6)/(X7-X6)))

```

```

C
C
C
      PRINTOUT OF THE COORDINATES AND THE SHAPE FACTORS.

```

```

      WRITE(6,45) DFU,DCC,S
45  FORMAT(/30X,'COORDINATES OF THE NODES'//15X,'DFU=',F6.4,
      < 10X,'DCC=',F6.4,10X,'S=',F6.4//)
      WRITE(6,50) X1,Y1,X2,Y2,X3,Y3,X4,Y4,X5,Y5,X6,Y6,X7,Y7,X8,Y8,X9,Y9
50  FORMAT(15X,'NODE NUMBER',5X,'X COORDINATE',9X,'Y COORDINATE'//20X,
      < '1',10X,E11.5,10X,E11.5/20X,'2',10X,E11.5,10X,E11.5/20X,'3',10X,
      < E11.5,10X,E11.5/20X,'4',10X,E11.5,10X,E11.5/20X,'5',10X,E11.5,10X
      < ,E11.5/20X,'6',10X,E11.5,10X,E11.5/20X,'7',10X,E11.5,10X,E11.5/
      < 20X,'8',10X,E11.5,10X,E11.5/20X,'9',10X,E11.5,10X,E11.5/)
      WRITE(6,55)
55  FORMAT(1H1,2X////////)

```

```

WRITE(6,60) S45,S14,S15,S12M,S12F,S25,S26,S23M,S23F,S56,S58,S89,
< S68,S36,S67,S69,S37,S79
60 FORMAT(22X,'SHAPE FACTORS.'////15X,'PATH',10X,'SHAPE FACTOR'//
< 15X,'S45',10X,E14.7/15X,'S14',10X,E14.7/15X,'S15',10X,E14.7/
< 15X,'S12M', 9X,E14.7/15X,'S12F', 9X,E14.7/15X,'S25',10X,E14.7/
< 15X,'S26',10X,E14.7/15X,'S23M', 9X,E14.7/15X,'S23F', 9X,E14.7
< /15X,'S56',10X,E14.7/15X,'S58',10X,E14.7/15X,'S89',10X,E14.7/
< 15X,'S68',10X,E14.7/15X,'S36',10X,E14.7/15X,'S67',10X,E14.7/
< 15X,'S69',10X,E14.7/15X,'S37',10X,E14.7/15X,'S79',10X,E14.7///)

```

```

C
C
C
      MASS FLOW RATE CALCULATION.

```

```

      MDOT=GIN*PI*DCO**2/4.0

```

```

C
C
C
      SELECTION OF AXIAL CALCULATION INCREMENT.

```

```

      DELL=H/50.0

```

```

C
C
C
      CALCULATION OF PRESSURE LOSS AT INLET OF CORE.

```

```

      RHO=PIN*144.0/(TIN+460.0)/386.0

```

```

      UB=GIN/RHO/3600.0

```

```

      RE=UB*DCO*RHO/VIS(TIN)*3600.0

```

```

      F=0.184/RE**0.2

```

```

      DELPF=F*DELL*RHO*UB**2/DCO/2.0/32.2*10.0

```

```

      DELPE=0.5*RHO*UB**2/2.0/32.2

```

```

C
C
C
      PRINTOUT OF CORE INLET CONDITIONS.

```

```

      WRITE(6,65)

```

```

65 FORMAT(15X,'AT THE INLET OF THE CORE'//)

```

```

      WRITE(6,70) UB,RE,F

```

```

70 FORMAT(15X,'CHANNEL AVE. VELOCITY ',2X,'REYNOLDS #',3X,'FRICTION F
<ACTOR'/21X,'(FT/SEC)'/21X,F6.2,12X,F8.1,8X,F7.4//)
WRITE(6,75)
75 FORMAT('*****
<*****
<',//)

```

C  
C  
C  
PRINTOUT OF COLUMN HEADINGS.

```

80 FORMAT(1H1,2X////////15X,'NO',7X,'Z-LOC',5X,'TO',6X,'T1/4',5X,
<'T1/2',5X,'T3/4',7X,'TF'/20X,'TN(1)',4X,'TN(2)',4X,'TN(3)',4X,
<'TN(4)',4X,'TN(5)',4X,'TN(6)'/15X,'TN(7)',4X,'TN(8)',4X,'TN(9)',
<5X,'TSURF',4X,'TBULK',4X,'HTCOF',5X,'DELP'//)
WRITE(6,80)

```

C  
C  
C  
CALCULATION OF CONDITIONS AT BEGINNING OF FIRST INCREMENT.

```

P1=PIN-(DELPE+DELPF)/144.0
T81=TIN
INC=1

```

C  
C  
C  
CALCULATION OF AXIAL COORDINATE OF CENTER OF FIRST INCREMENT.

```

ZC= H/2.0-DELL/2.0

```

C  
C  
C  
C  
C  
INITIAL GUESS OF AVERAGE FUEL AND MODERATOR TEMPERATURES FOR  
THE FIRST INCREMENT. THESE ARE USED TO EVALUATE THE THERMAL-  
CONDUCTIVITIES IN THE CALCULATION OF THE MODERATOR TEMPERATURE  
DISTRIBUTION.

```

TMAV=TIN+300.0*COS(PI*ZC/HE)
TFDAV=TIN+500.0*COS(PI*ZC/HE)

```



C  
C  
C  
CALCULATION OF AVERAGE BULK TEMPERATURE FOR INCREMENT.

85 QTPAV=QTPG\*COS(PI\*ZC/HE)  
TB2=TB1+QTPAV\*PI\*DFU\*\*2.0\*DELL/4.0/MDOT/1.24800\*2.0

C  
C  
C  
C  
C  
THE MULTIPLICATION BY 2 IN THE PREVIOUS CALCULATION IS REQUIRED  
BECAUSE TWICE THE ENERGY GENERATED IN ONE FUEL ROD ENTERS EACH  
COOLANT CHANNEL.

TBAV=(TB1+TB2)/2.0

C  
C  
C  
CALCULATION OF PRESSURE DROP AND EXIT PRESSURE FOR INCREMENT.

RHO=PI\*144.0/(TBAV+460.0)/386.0  
UB=GIN/RHO/3600.0  
RE=UB\*DCO\*RHO/VIS(TBAV)\*3600.0  
F=0.184/RE\*\*0.2  
DELPF=F\*DELL\*RHO\*UB\*\*2/DCO/2.0/32.2  
P2=P1-DELPF/144.0

C  
C  
C  
CALCULATION OF HEAT TRANSFER COEFFICIENT FOR INCREMENT.

PR=1.248\*VIS(TBAV)/KBC(TBAV)  
NU=0.023\*RE\*\*0.8\*PR\*\*0.4  
HTC=NU\*KBC(TBAV)/DCO

C  
C  
C  
C  
C  
CALCULATION OF TEMPERATURE DISTRIBUTION IN GRAPHITE MODERATOR.

C  
OBTAINING THE BEST GUESSES FOR AVERAGE FUEL AND MODERATOR

C TEMPERATURES FOR FINITE-DIFFERENCE CALCULATION OF MODERATOR  
C TEMPERATURE DISTRIBUTION.  
C

IF(INC.EQ.1) GO TO 95  
TMAV=TBAV+(TMAV-TBAV)\*CTPAV/QTPCLD  
TFJAV=TBAV+(TFJAV-TBAV)\*QTPAV/QTPCLD  
95 RATIO=KFU(TFJAV)/KMG(TMAV)

C  
C CALCULATING THE MAIN DIAGONAL COEFFICIENTS FOR THE COEFFICIENT  
C MATRIX OF THE NODAL EQUATIONS.  
C

S1=S14+S15+S12M+RATIO\*S12F  
S2=S26+S25+S12M+S12F\*RATIO+S23M+RATIO\*S23F  
S3=S36+S37+S23M+RATIO\*S23F  
S4=S14+S45  
S5=S45+S15+S25+S56+S58  
S6=S56+S26+S36+S67+S69+S68  
S7=S37+S67+S79+PI\*DCO\*HTC/(24.0\*KMG(TMAV))  
S8=S58+S68+S89  
S9=S89+S69+S79+(PI\*DCO\*HTC/(24.0\*KMG(TMAV)))

C  
C SETTING UP THE COEFFICIENT MATRIX FOR SIMQ SOLUTION OF NODAL-  
C EQUATIONS.  
C

DO 100 I=1,9  
100 B(I)=0.0  
DO 105 I=1,81  
105 A(I)=0.0  
A(1)=-S1  
A(10)=(S12M+RATIO\*S12F)  
A(28)=S14  
A(37)=S15

A(2)=A(10)  
A(11)=-S2  
A(20)=(S23M+RATIO\*S23F)  
A(38)=S25  
A(47)=S26  
A(12)=A(20)  
A(48)=S36  
A(57)=S37  
A(21)=-S3  
A(4)=S14  
A(40)=S45  
A(31)=-S4  
A(5)=S15  
A(14)=S25  
A(50)=S56  
A(68)=S58  
A(41)=-S5  
A(32)=S45  
A(42)=S56  
A(15)=S26  
A(24)=S36  
A(60)=S67  
A(78)=S69  
A(69)=S68  
A(51)=-S6  
A(25)=S37  
A(52)=S67  
A(79)=S79  
A(61)=-S7  
A(71)=-S8  
A(44)=S58  
A(53)=S68

```

A(80)=S89
A(81)=-S9
A(72)=S89
A(54)=S69
A(63)=S79
B(1)=-QTPAV*PI*DFU**2/(96.0*KMU(TMAV))
B(2)=2.0*B(1)
B(3)=B(1)
B(7)=-PI*DCU*HTC*TBAV/(24.0*KMC(TMAV))
B(9)=B(7)
NNN=9
KKS=0

```

```

C
C     USING SIMQ TO OBTAIN SOLUTION OF NODAL EQUATIONS.
C

```

```

CALL SIMQ(A,B,NNN,KKS)
DO 110 I=1,9
110 T(I)=B(I)

```

```

C
C     CALCULATION OF AVERAGE TEMPERATURE AT SURFACES OF FUEL AND
C     COOLANT FOR INCREMENT.
C

```

```

TF=(T(1)+2.0*T(2)+T(3))/4.0
TSAV=(T(7)+T(9))/2.0

```

```

C
C     CALCULATION OF TEMPERATURE AT CENTER OF FUEL FOR INCREMENT. AN
C     ITERATION TECHNIQUE IS USED TO OBTAIN FUEL THERMAL CONDUCTIVITY
C     WITHIN 2%.
C

```

```

KFJ1=KFU(TF)
115 TU=TF+QTPAV*DFU**2.0/16.0/KFU1
TFAVS=(TF+TC)/2.0

```

```
KFU2=KFU(TFAVS)
ERR=ABS((KFU1-KFU2)/KFU2)
IF(ERR-0.02 )125,125,126
120 KFU1=KFU2
GO TO 115
```

```
C
C      SAVING VALUES OF THERMAL CONDUCTIVITIES FOR LATER COMPARISONS.
C
```

```
125 COMPA1=KFU(TFOAV)
    COMPA2=KMO(TMAV)
```

```
C
C      CHECK TO DETERMINE IF CORRECT MODERATOR AND FUEL THERMAL-
C      CONDUCTIVITIES WERE USED IN MODERATOR FINITE-DIFFERENCE
C      CALCULATIONS. IF NOT, AN ITERATION ON THE AVERAGE THERMAL-
C      CONDUCTIVITIES IS PERFORMED.
C
```

```
TFOAV=3.0/8.0*TO+5.0/8.0*TF
TMAV=(T(1)+T(2)+T(3)+T(4)+T(5)+T(6)+T(7)+T(8)+T(9))/9.0
RAT1=ABS((COMPA1-KFU(TFOAV))/COMPA1)
RAT2=ABS((COMPA2-KMO(TMAV))/COMPA2)
IF(RAT1.LE.0.02.AND.RAT2.LE.0.02) GO TO 130
GO TO 95
```

```
C
C      CALCULATION OF FUEL TEMPERATURE AT 1/4, 1/2, AND 3/4 FUEL RADII
C      FOR INCREMENT.
C
```

```
130 T14=TO-QTPAV*DFU**2.2/16.0/KFU1/16.0
    T12=TO-QTPAV*DFU**2/16.0/KFU1/4.0
    T34=TC-QTPAV*DFU**2.0/16.0/KFU1/16.0*9.0
```

```
C
C      PRINTOUT OF RESULT FOR CALCULATION INCREMENT.
C
```

```

C
WRITE(6,135) INC,ZC,TD,T14,T12,T34,TF,B,TSBV,TBAV,HTC,DELPF
135 FORMAT(15X,I2,7X,F7.3,2X,F6.1,4X,F6.1,3X,F6.1,3X,F6.1,4X,F6.1/
<20X,F6.1,5(3X,F6.1)/15X,3(F6.1,3X),1X,F6.1,2(3X,F6.1),4X,F6.2/)
IF(INC.EQ.11.OR.INC.EQ.23.OR.INC.EQ.35.OR.INC.EQ.47) WRITE(6,55)

```

```

C
CHECK TO SEE IF CALCULATIONS HAVE BEEN COMPLETED FOR ENTIRE
CORE.

```

```

IF(INC-50) 140,145,145

```

```

C
SETTING CONDITIONS FOR BEGINNING OF NEXT CALCULATION INCREMENT.

```

```

140 INC=INC+1
ZC=ZC-DELL
TB1=TB2
P1=P2
QTPOLD=QTPAV

```

```

C
TRANSFERRING TO START CALCULATIONS FOR NEXT INCREMENT.

```

```

GO TO 85

```

```

C
CALCULATION OF CORE EXIT CONDITIONS OF COOLANT.

```

```

145 RHO=P2*144.C/(TB2+460.0)/386.0
UB=GIN/RHO/3600.0
RE=UB*DCO*KHO/VIS(TB2)*3600.0
F=0.184/RE**0.2
DELPF=F*DELL*RHO*UB**2/DCO/2.0/32.2*10.0
DELPE=RHO*UB**2/2.0/32.2
PEX=P2-(DELPE+DELPF)/144.0

```



TEX=TB2

C  
C  
C

PRINTOUT OF CORE EXIT COOLANT CONDITIONS.

WRITE(6,75)

WRITE(6,150)

150 FORMAT(/,15X,'EXIT PRESSURE',10X,'EXIT TEMPERATURE',/19X,  
<'(PSIA)',18X,' (F)'/)

WRITE(6,155)PEX,TEX

155 FORMAT(18X,F6.1,18X,F6.1)

C  
C  
C  
C  
C

CALCULATION OF AVERAGE POWER OF FUEL ROD IN KW/FT.

PRINTOUT OF AVERAGE POWER.

POVL=QTPO\*HE\*DFU\*\*2/2.0\*SIN(PI\*H/2.0/HE)/H

POVL=POVL/3412

WRITE(6,160)POVL

160 FORMAT(/15X,'POWER PER UNIT LENGTH (KW/FT) :',F6.2/////)

WRITE(6,75)

WRITE(6,55)

STOP

END

C  
C  
C  
C  
C  
C  
C  
C  
C  
C

.....

SUBROUTINE SIMQ

PURPOSE

OBTAIN SOLUTION OF A SET OF SIMULTANEOUS LINEAR EQUATIONS,  
AX=B

USAGE

C CALL SIMQ(A,B,N,KS)

C DESCRIPTION OF PARAMETERS

C A - MATRIX OF COEFFICIENTS STORED COLUMNWISE. THESE ARE  
C DESTROYED IN THE COMPUTATION. THE SIZE OF MATRIX A IS  
C N BY N.

C B - VECTOR OF ORIGINAL CONSTANTS (LENGTH N). THESE ARE  
C REPLACED BY FINAL SOLUTION VALUES, VECTOR X.

C N - NUMBER OF EQUATIONS AND VARIABLES. N MUST BE .GT. ONE.

C KS - OUTPUT DIGIT

C 0 FOR A NORMAL SOLUTION

C 1 FOR A SINGULAR SET OF EQUATIONS

C REMARKS

C MATRIX A MUST BE GENERAL.

C IF MATRIX IS SINGULAR , SOLUTION VALUES ARE MEANINGLESS.

C AN ALTERNATIVE SOLUTION MAY BE OBTAINED BY USING MATRIX  
C INVERSION (MINV) AND MATRIX PRODUCT (GMPRD).

C SUBROUTINES AND FUNCTION SUBPROGRAMS REQUIRED

C NONE

C METHOD

C METHOD OF SOLUTION IS BY ELIMINATION USING LARGEST PIVOTAL  
C DIVISOR. EACH STAGE OF ELIMINATION CONSISTS OF INTERCHANGING  
C ROWS WHEN NECESSARY TO AVOID DIVISION BY ZERO OR SMALL  
C ELEMENTS.

C THE FORWARD SOLUTION TO OBTAIN VARIABLE N IS DONE IN  
C N STAGES. THE BACK SOLUTION FOR THE OTHER VARIABLES IS  
C CALCULATED BY SUCCESSIVE SUBSTITUTIONS. FINAL SOLUTION  
C VALUES ARE DEVELOPED IN VECTOR B, WITH VARIABLE 1 IN B(1),  
C VARIABLE 2 IN B(2),....., VARIABLE N IN B(N).



```

C           IF NO PIVOT CAN BE FOUND EXCEEDING A TOLERANCE OF 0.0,
C           THE MATRIX IS CONSIDERED SINGULAR AND KS IS SET TO 1. THIS
C           TOLERANCE CAN BE MODIFIED BY REPLACING THE FIRST STATEMENT.
C
C           .....
C
C           SUBROUTINE SIMQ(A,B,N,KS)
C           DIMENSION A(81),B(9)
C
C           FORWARD SOLUTION
C
C           TOL=0.0
C           KS=0
C           JJ=-N
C           DO 65 J=1,N
C           JY=J+1
C           JJ=JJ+N+1
C           BIGA=0
C           IT=JJ-J
C           DO 30 I=J,N
C
C           SEARCH FOR MAXIMUM COEFFICIENT IN COLUMN
C
C           IJ=IT+I
C           IF(ABS(BIGA)-ABS(A(IJ))) 20,30,30
C           20 BIGA=A(IJ)
C           IMAX=I
C           30 CONTINUE
C
C           TEST FOR PIVOT LESS THAN TOLERANCE (SINGULAR MATRIX)
C
C           IF(ABS(BIGA)-TOL) 35,35,40

```

```
35 KS=1  
    RETURN
```

```
C  
C  
C
```

```
    INTERCHANGE ROWS IF NECESSARY
```

```
40 I1=J+N*(J-2)  
    IT=IMAX-J  
    DO 50 K=J,N  
        I1=I1+N  
        I2=I1+IT  
        SAVE=A(I1)  
        A(I1)=A(I2)  
        A(I2)=SAVE
```

```
C  
C  
C
```

```
    DIVIDE EQUATION BY LEADING COEFFICIENT
```

```
50 A(I1)=A(I1)/BIGA  
    SAVE=B(IMAX)  
    B(IMAX)=B(J)  
    B(J)=SAVE/BIGA
```

```
C  
C  
C
```

```
    ELIMINATE NEXT VARIABLE
```

```
    IF(J-N) 55,70,55  
55 IQS=N*(J-1)  
    DO 65 IX=JY,N  
        IXJ=IQS+IX  
        IT=J-IX  
        DO 60 JX=JY,N  
            IXJX=N*(JX-1)+IX  
            JJX=IXJX+IT  
60 A(IXJX)=A(IXJX)-(A(IXJ)*A(JJX))
```

```

05 B(IX)=B(IX)-(B(J)*A(IXJ))
C
C     BACK SCLUTION
C
70 NY=N-1
   IT=N*N
   DO 80 J=1,NY
   IA=IT-J
   IB=N-J
   IC=N
   DO 80 K=1,J
   B(IB)=B(IB)-A(IA)*B(IC)
   IA=IA-N
80 IC=IC-1
   RETURN
   END

```

6.0 References

1. Glasstone, S., and M. C. Edlund, The Elements of Nuclear Reactor Theory, D. Van Nostrand Co., Inc., Princeton, N.J., 1952.
2. Zweifel, P. F., Reactor Physics, McGraw-Hill Book Company, New York, N.Y., 1973.
3. Glasstone, S., and A. Sesonske, Nuclear Reactor Engineering, D. Van Nostrand Co., Inc., Princeton, N.J., 1963.
4. El-Wakil, M. M., Nuclear Heat Transport, International Textbook Company, Scranton, Pa., 1971.
5. Holman, J. P., Heat Transfer, Third Edition, McGraw-Hill Book Company, New York, N.Y., 1972.
6. Kreith, F., Principles of Heat Transfer, Third Edition, Intext Educational Publishers, New York, N.Y., 1973.
7. Baumeister, T., and L. S. Marks, Standard Handbook for Mechanical Engineers, McGraw-Hill Book Company, New York, N.Y., 1967.
8. Dusenberre, G. M., Heat-Transfer Calculations by Finite Differences, International Textbook Company, Scranton, Pa., 1961.
9. Shames, I. H., Mechanics of Fluids, McGraw-Hill Book Company, New York, N.Y., 1962.
10. Sabersky, R. H., and A. J. Acosta, Fluid Flow, the Macmillan Company, New York, N.Y., 1964.
11. Flow of Fluids Through Valves, Fittings, and Pipe, Technical Paper No. 410, Crane Company, Chicago, Ill., 1965.
12. Dittus, F. W., and L. M. K. Boelter, University of California Publs. Eng., Vol. 2, 1930, p. 443.

7.0 Problems

1. By performing an energy balance on a differential element with sides  $dx$ ,  $dy$ , and  $dz$ , derive the steady state heat conduction equation in Cartesian coordinates.
2. Derive the steady state heat conduction equation in cylindrical coordinates.
3. Develop an expression for the temperature distribution in a long, thin, hollow cylindrical fuel rod with inner radius  $r_i$ , outer radius  $r_o$ , and volumetric thermal source strength  $q'''$ . Assume that the inner surface is insulated and at temperature  $T_i$ .
4. A long, thin, hollow cylindrical fuel rod with volumetric thermal source strength  $q'''$  is cooled on both the inner and outer surfaces ( $r = r_i$  and  $r = r_o$  surfaces) such that the surface temperatures are  $T_i$  and  $T_o$ , respectively. Derive an expression for the location of the maximum temperature in the fuel.
5. Calculate the ratio of peak power to average power for a fuel rod of constant cross section assuming that the volumetric thermal source strength varies as  $q''' = q'''_0 \cos(\pi Z/H_c)$  and that the extrapolation length is 10% of the core height. Compare this ratio to that for the case where the extrapolation length is assumed to be zero.
6. Develop an expression for the steady state heat transfer rate through a cylindrical shell of inside radius  $r_i$  and outside radius  $r_o$  with no internal energy generation. Your expression should contain only the outside surface temperature  $T_o$ , the inside surface temperature  $T_i$ , the thermal conductivity  $k$ , the length of the shell  $\Delta L$ ,  $r_i$ , and  $r_o$ .
7. A HTGR fuel rod is 0.6 in. in diameter and 30 in. long. The surface temperature of the rod is at 1200 F and the volumetric thermal source strength of the rod is  $8 \times 10^6$  Btu/hr-ft<sup>3</sup>. The thermal conductivity is 12.0 Btu/hr-ft-F. Determine the temperature and heat transfer rate at  $r = 0.2$  in.
8. The fuel rod in Problem 7 fits inside a fuel hole that is 0.630 in. in diameter. The 0.030 in. diametrical gap between the fuel rod and moderator is filled with helium gas. Assuming that the heat transfer through the helium is by molecular conduction only ( $k_{He} = 0.140$  Btu/hr-ft-F) determine the temperature difference between the fuel and moderator surfaces.
9. Develop the steady state finite-difference nodal equation for node 2 of Figure 2.
10. Develop the steady state finite-difference nodal equation for node 4 of Figure 2.

11. Develop the steady state finite-difference nodal equation for node 10 of Figure 2.
12. Develop the steady state finite-difference nodal equation for node E of Figure 3.
13. Develop the steady state finite-difference nodal equation for node H of Figure 3.
14. Develop the steady state finite-difference nodal equation for node J of Figure 3.
15. A 25 foot long HTGR core contains 0.520 in. diameter coolant holes. The average conditions in the core are 500 psia and 1000 F. The mass velocity of the helium is  $2.0 \times 10^5$  lbm/hr-ft<sup>2</sup>. Determine the pressure drop through the core.
16. Determine the effect on pressure drop of a 20% decrease in coolant hole diameter for the core in Problem 15. Assume the coolant conditions and mass velocity remain the same.
17. Determine the heat transfer coefficient for the flow conditions of Problem 15.
18. A HTGR core contains 0.75 in. diameter coolant holes through which helium flows. At a particular location in the core the pressure is 500 psia, the temperature is 900 F and the coolant velocity is 216 ft/sec. Determine the heat transfer coefficient.
19. In a HTGR core the volumetric thermal source strength varies axially as  $q'''(Z) = q_o''' \cos(\pi Z/H_e)$ . The energy generated in each two fuel rods is removed by a coolant channel which has a mass flow rate of  $\dot{m}$  and an inlet temperature of  $T_{in}$ . Designate the fuel diameter as  $D_f$  and the coolant hole diameter as  $D_c$ . Develop an expression for the axial variation of the temperature at the surface of the moderator. Your expression should contain only  $T_{in}$ ,  $q_o'''$ ,  $D_f$ ,  $D_c$ ,  $H$ ,  $H_e$ ,  $\dot{m}$ ,  $C_p$ ,  $h$ , and  $Z$ .
20. From the expression developed in Problem 19 determine the axial location where the moderator surface temperature (moderator-coolant interface) is a maximum.
21. A 4000 Mw (t) HTGR contains 5400 right hexagonal prism fuel elements each 14.2 in. across the flats and 31.2 in. long. The fuel elements are stacked 8 high in the core. The uranium-thorium fuel in carbide form is contained in 0.62 in. diameter fuel holes. The core is cooled by the downward flow of helium through 0.825 in. diameter coolant holes. The helium enters at 600 F, 725 psia, and with an average mass velocity of  $8.3 \times 10^4$  lbm/hr-ft<sup>2</sup>. Each fuel element assembly contains 132 fuel holes. The spacing between the fuel and coolant holes in the element is 1.112 in. The thermal source strength varies as  $q''' = q_o''' \cos \pi Z/H_e$  and  $H_e = 1.1H$ . Determine

the maximum fuel temperature and the maximum moderator temperature in the core.

22. Determine the % increase in power that would produce a 1800 F maximum fuel temperature for the core and flow conditions of Problem 21.
23. Determine the % reduction in core flow that would produce a 1800 F maximum fuel temperature for the core and flow conditions of Problem 21.
24. A 2000 Mw (t) HTGR contains 2400 right hexagonal prism fuel assemblies stacked 10 elements high to form the core. Each fuel element is 12 in. across the flats and 30 in. high. In each element the uranium-thorium fuel in carbide form is contained in 150 fuel holes each 0.48 in. in diameter. The core is cooled by the downward flow of helium through 0.56 in. coolant holes. The helium enters at 700 F, 600 psia, and with an average velocity of 300 ft/sec. The spacing between the fuel and coolant holes is 0.80 in. The axial power distribution is a truncated cosine function with an extrapolation length of 16 in. Determine the location and magnitude of the maximum fuel, moderator, and coolant temperatures.
25. The coolant holes in one of the fuel element assembly columns of the core in Problem 24 are undersized by 30%. Determine the % increase in maximum fuel, moderator, and coolant temperatures over those for the normal reactor fuel element assemblies.
26. Determine the % overpower that leads to a maximum fuel temperature of 1800 F for the core and flow conditions of Problem 24.